Two Novel *S*-methyltransferases Confer Dimethylsulfide Production in *Actinomycetota*

Ruihong Guo, Zihua Guo, Yi Zhou, Yunhui Zhang, Haojin Cheng, Rebecca Devine, Chuang Sun, Ronghua Liu, Yanfen Zheng, Andrew J. Gates, Jonathan D. Todd, Xiao-Hua Zhang**

R. Guo, Z. Guo, Y. Zhou, Y. Zhang, H. Cheng, R. Liu, J. D. Todd, X.-H. Zhang
Frontiers Science Center for Deep Ocean Multispheres and Earth System, and College of Marine Life Sciences, Ocean University of China, Qingdao, China
E-mail: jonathan.todd@uea.ac.uk; xhzhang@ouc.edu.cn

R. Guo, X.-H. Zhang
Laboratory for Marine Ecology and Environmental Science, Qingdao Marine Science and Technology Center, Qingdao, China

Z. Guo, Y. Zhang, X.-H. Zhang
Key Laboratory of Evolution & Marine Biodiversity (Ministry of Education), and Institute of Evolution & Marine Biodiversity, Ocean University of China, Qingdao, China

R. Devine, C. Sun, A. J. Gates, J. D. Todd
John Innes Centre, Department of Molecular Microbiology, and Centre for Microbial Interactions, Norwich Research Park, Norwich, United Kingdom

C. Sun, A. J. Gates, J. D. Todd
School of Biological Sciences, University of East Anglia, Norwich Research Park, Norwich, United Kingdom

Y. Zheng
Marine Agriculture Research Center, Tobacco Research Institute of Chinese Academy of Agricultural Sciences, Qingdao, China

Funding: National Natural Science Foundation of China (32370118, 42306115 and 42376101), National Key R&D Program of China (2025YFF0516900 and 2025YFF0516903), Shandong Provincial Natural Science Foundation

(ZR2023QD017), China Postdoctoral Science Foundation (2022M722975), the Postdoctoral Innovation Program of Shandong Province (SDCX-ZG-202201016), the Biotechnology and Biological Sciences Research Council, UK (BB/X005968), Natural Environmental Research Council, UK (NE/P012671) and China Scholarship Council (No. 202106330012).

Keywords: Dimethylsulfide, Methanethiol, Sulfide, *S*-methyltransferase, *Actinomycetota*

Abstract

Hydrogen sulfide (H_2S), methanethiol (MeSH) and dimethylsulfide (DMS) are abundant sulfur gases with crucial roles in global sulfur and nutrient cycling, chemotaxis, and climate regulation. Microorganisms can *S*-methylate H_2S and MeSH, which can be cytotoxic, to yield non-toxic DMS via MddA or MddH enzymes in largely terrestrial or marine environments, respectively. However, many important and abundant bacteria, e.g. *Actinomycetota*, contain unknown Mdd enzymes, thus the potential of these pathways is underestimated. Here, we identify two novel *S*-adenosine-methionine (SAM)-dependent H_2S and MeSH *S*-methyltransferases, MddM1 and MddM2, in the DMS-producing actinomycete *Mycolicibacterium poriferae* ZYF656, isolated from the Mariana Trench. *M. poriferae* ZYF656 MddM1 and MddM2 likely detoxify H_2S and MeSH and alleviate oxidative stress, since *mddM1* and *mddM2* transcription is induced by H_2S, MeSH and oxidative stress, and their expression in *Escherichia coli* enhances H_2S, MeSH and oxidative stress tolerance. MddM1 and/or MddM2 are in > 50% of *actinomycetota*, including the model *Streptomyces* species, *S. venezuelae*, but are also seen in some *Chloroflexota*, *Acidobacteriota* and *Proteobacteria*. *mddM1* is always more abundant than *mddM2* in diverse environments and is prevalent in soils and marsh sediments. This study highlights the significance of H_2S- and MeSH-dependent DMS production and, principally, of *Actinomycetota* in global DMS production and sulfur cycling.

Ruihong Guo, Zihua Guo, Yi Zhou and Yunhui Zhang contributed equally to this work.

1 Introduction

Dimethylsulfide (DMS) is Earth's major biogenic sulfur compound transferred from marine environments to the atmosphere, representing 13-37 Tg sulfur annually. [1-4] Atmospheric DMS and related compounds, like methanethiol (MeSH), can be oxidized to form cloud condensation nuclei (CCN) and impact the climate.[5-7] Furthermore, DMS is a nutrient and a signaling molecule for diverse microorganisms.[8-9]

In marine environments, most DMS is thought to arise from the microbial cleavage of the abundant osmolyte dimethylsulfoniopropionate (DMSP) via diverse DMSP lyase enzymes.[10] However, DMS can also result from the enzymatic degradation of dimethyl sulfoxide (DMSO), methoxyaromatic compounds,[11] or from *S*-methylation of MeSH or hydrogen sulfide (H_2S).[12-15] H_2S is a toxic volatile, often present in diverse environments, e.g., hydrothermal vents and sediments, at millimolar concentrations.[16-17] MeSH, another toxic volatile, is a potentially abundant by-product of DMSP demethylation, which accounts for up to 80% of marine DMSP catabolism (**Figure 1A**).[18] In this pathway, DMSP is demethylated to 3-methylmercaptopropionate (MMPA) via DmdA, predicted in 20% of marine bacteria.[19-20] MMPA can be further processed to MeSH via *dmdB/C/D* gene products which are ubiquitous in marine and terrestrial bacteria (Figure 1A).[19-20] MeSH can also result from DMS and methionine (Met) degradation via DMS monooxygenase DmoA and Met-gamma-lyase enzymes MegL, respectively (Figure 1A).[21-23] Thus, there are many DMSP-independent routes to DMS, and the substrates for these pathways, particularly H_2S and MeSH, are often abundant in marine and terrestrial environments.

Previous studies identified TMT1A and TMT1B as thiol methyltransferase enzymes capable of methylating H_2S in humans, other mammals and fish.[24-25] Furthermore, diverse microorganisms utilized enzymes, termed MddA and MddH, to *S*-methylate H_2S and MeSH yielding DMS in reactions where *S*-adenosine methionine (SAM) was the methyl donor (Figure 1A).[14-15] These Mdd enzymes were proposed to detoxify H_2S and MeSH via production of non-toxic DMS.[14-15] MddA, a membrane-associated enzyme, was predominantly found in terrestrial actinobacteria, cyanobacteria, rhizobiales, pseudomonads, and some marine algae.[26] In contrast, MddH was shown

to be a cytoplasmic enzyme and widespread in diverse marine bacteria, especially *Gammaproteobacteria*.[15] The genetic potential to *S*-methylate H_2S and MeSH was found to be sizable in diverse marine (largely via MddH) and terrestrial (largely via MddA) environments, particularly in sediments, where H_2S and MeSH concentrations were likely higher.[16-17] Although *mddH* was abundant in marine multi-omics data, it was never more abundant than DMSP lyase genes.[15] These findings implied that microbial *S*-methylation of H_2S and MeSH played important roles in microbial stress responses and global DMS production, but less so than DMSP cleavage in marine settings. However, there were still bacteria which *S*-methylated H_2S and MeSH but lacked MddA and MddH and thus contained novel enzymes.[12-13, 15]

Here, we screened cultivable bacteria from the Mariana Trench, previously reported to exhibit high Mdd activity,[27] for isolates that *S*-methylated H_2S and MeSH. One such isolate, the actinomycete *Mycolicibacterium poriferae* ZYF656, was able to *S*-methylate H_2S and MeSH but lacked all known *mdd* genes, *TMT1A* and *TMT1B*, implying it contained novel Mdd enzymes. We identified and characterized two novel enzymes responsible for H_2S and MeSH *S*-methylation, their role in bacteria and implied importance in stress tolerance, global DMS production and sulfur cycling.

2 Results

2.1 DMS and MeSH production by *Mycolicibacterium poriferae* ZYF656

We noted that *M. poriferae* ZYF656, a new species isolated from the 9,600 m deep Mariana Trench seawater, produced DMS when incubated with Met, MMPA, H_2S and MeSH (Figure 1B). This actinobacterium did not produce DMSP even when grown in the presence of Met (the universal DMSP precursor), and it failed to produce DMS or MeSH when incubated with DMSP (Figure 1B). These data confirmed that *S*-methylation of H_2S and MeSH, rather than DMSP-dependent pathways were the source of DMS produced by this marine actinobacterium.

The *M. poriferae* ZYF656 genome (GenBank accession number: CP151154) lacked both identifiable DMSP demethylase (*dmdA*) and DMSP lyase (*ddd*) genes (Figure 1A),

consistent with its absence of DMSP lyase and demethylation activity. However, *M. poriferae* ZYF656 did contain *megL* and *dmdB/AcuH*, whose Met-gamma-lyase (EC4.4.1.11) and DMSP demethylation pathway protein products can generate MeSH from Met and MMPA, respectively (Figure 1A, Table S1, Supporting information). These findings are consistent with the data shown in Figure 1B, supporting the proposed role of Met and MMPA as precursors for DMS production via MeSH *S*-methylation. Interestingly, the predicted *M. poriferae* ZYF656 proteome lacked any obvious MddA, MddH, TMT1A or TMT1B homologues at ≥ 40% amino acid identity, implying that this actinobacterium may utilize novel Mdd enzymes for H_2S and MeSH *S*-methylation.

2.2 Identification of the novel enzymes MddM1 and MddM2

To identify the genes responsible for H_2S and MeSH *S*-methylation, a genomic library of *M. poriferae* ZYF656 was constructed and screened in *Escherichia coli* JM109 for Mdd activity. Two distinct clones with Mdd activity were identified and sequenced. Each clone contained a distinct SAM-dependent methyltransferase, termed MddM1 (PP661493) and MddM2 (PP661494). When cloned and expressed in *E. coli* BL21 (DE3), *mddM1* and *mddM2* each conferred the ability to *S*-methylate H_2S to MeSH and DMS, as well as MeSH to DMS (Figure 1C,D). Furthermore, cloned *mddM1* and *mddM2* each also conferred MeSH-dependent DMS production from 1 mM MeSH and H_2S to *Corynebacterium glutamicum* RES167, an actinobacterium lacking the Mdd pathway (Figure S1A,B, Supporting information).

MddM1 and MddM2 were similar-sized proteins comprising 210 and 204 amino acids with predicted molecular weights of ~23 kDa and ~21 kDa, respectively. However, their theoretical *p*I values were quite different being 5.88 for MddM1 and 7.86 for MddM2. MddM1 was an UbiG family (COG2227) SAM-dependent methyltransferase, predicted by CELLO to be cytoplasmic with no signal peptide. Like MddH,[15] MddM2 was a UbiE family SAM-dependent methyltransferase, but by contrast it was predicted to be membrane-bound (by CELLO), like MddA,[14] with a transmembrane helix (by TMHMM) and a SEC signal peptide whose cleavage site was likely between position

residues 41 and 42 as determined by SignalP 6.0.[28] Indeed, *M. poriferae* ZYF656 MeSH *S*-methylation activity was found to be both cytosolic (1.34 ± 0.32 pmol DMS mg^{-1} total protein h^{-1}) and membranous (0.17 ± 0.01 pmol DMS mg^{-1} total protein h^{-1}), consistent with the higher activity of the MddM1 protein and lower activity of the MddM2 protein.

Sequence alignment of MddM1 and MddM2 with other characterized SAM-dependent *S*-methyltransferases, including microbial MddH and human TMT1A and TMT1B, revealed that they shared extended residue similarity including the conserved GxGxG motif for SAM binding (Figure S2A, Supporting information).[15] Further structural modelling, using AlphaFold3,[29] showed MddM1 and MddM2 also shared structural similarity with each other and with other characterized SAM-dependent methyltransferases, but they have different N-terminal regions (Figure S2B, Supporting information). While the N-terminal region of MddM1 is predicted to adopt similar structure to MddH that is truncated relative to human SAM-dependent *S*-methyltransferases,[15] the N-terminal region of MddM2 is predicted to be an extended unstructured peptide region containing the putative SEC signal sequence. As MddM1 and MddM2 adopt a MddH-like fold, both are structurally distinct to the microbial integral membrane SAM-dependent S-methyltransferase MddA.[26]

2.3 MddM1 and MddM2 are abundant in *Actinomycetota*

The distribution of *mddM1* and *mddM2* in genomes available on the UniprotKB and Swiss-Prot database was analyzed to predict organisms with the potential to *S*-methylate H_2S and MeSH. Candidate MddM1 and MddM2 proteins (E-value ≤ e-30) were predominantly found in *Actinomycetota*, but also in some *Proteobacteria* (including *Alpha*-, *Beta*-, *Gamma*- and *Delta-proteobacteria*), *Chloroflexota*, *Myxococcota*, *Acidobacteriota*, *Desulfuromonadia*, and *Candidatus* Dormibacteraeota (**Figure 2**). These MddM1 homologues were predominantly from soil or marine environments, but were also seen, albeit less frequently, in bacteria from human, plant, animal, water and other sources. In contrast, only 24 MddM2 homologues were

identified, and all were *Actinomycetota* from human sources (Figure 2). Representative candidate MddM1 and MddM2 homologues from *Actinomycetota*, *Acidobacteriota*, *Deltaproteobacteria* and *Chloroflexota* were overexpressed in *E. coli* BL21 (DE3) and all showed H_2S- and MeSH-dependent DMS production, confirming the activity of these proteins (**Table 1**).

Focused analysis of 42,815 *Actinomycetota* genomes available on NCBI inferred H_2S and MeSH dependent DMS production to be important in this phylum, with 51.02%, 21.60%, 4.58% and 1.16% predicted to contain MddM1, MddA, MddH or MddM2, respectively (Figure S3, Supporting information). The majority of MddM1 homologues were from *Streptomyces*, *Mycobacterium* and *Mycolicibacterium* genera (Figure S3, Supporting information). Notably, *Streptomyces* are generally reported as fast growing bacteria, widely distributed in diverse environments, particularly soils, and 19.75% contained MddM1 (Figure S3, Supporting information).[30-31] These data implied that the *Actinomycetota*, particularly *Streptomyces* in soil and human environments may be significant producers of DMS via the *S*-methylation of H_2S and MeSH (Figure S3, Supporting information). However, we found that the model *Streptomyces*, *S. venezuelae* and its *mddM1* mutant derivative (generated here), made no DMS, even when incubated with Met or MeSH (Figure S1C,D, Supporting information). However, DMS production was detected when *mddM1* was expressed under control of an ectopic promoter in the *S. venezuelae mddM1*$^-$ grown in the presence of Met or MeSH (Figure S1C,D, Supporting information). These data implied that *S. venezuelae* did not express and utilise MddM1 under the tested conditions, as is common in *Streptomyces* secondary metabolite production systems.[32] It also further indicated the limitation of functional predictions based only on genetic potential.

Since some eukaryotic algae contain MddA,[14] we probed the Marine Microbial Eukaryote Transcriptome Sequencing Project (MMETSP) database with MddM1, MddM2 and MddH sequences.[33] This identified 14 proteins clustered in a distinct clade away from MddM1 and MddH, and no MddM2 homologs (Figure S4, Supporting information). To establish if the distinct clade of Mdd-like proteins had H_2S or MeSH

S-methylation activity, a representative from a liverwort *Riccia sorocarpa* (MMETSP0818 10907|m. 27989) with 41.30% amino acid identity, 95% coverage and an E-value of 2.68e-34 to MddM1 (MDE3069982.1 *Acidobacteriota* bacterium), was chosen for characterisation. This candidate gene was codon optimized for expression in *E. coli*, cloned into pET-24a and expressed in *E. coli* BL21 (DE3), but despite a soluble protein product being overproduced, it conferred no H_2S or MeSH *S*-methyltransferase activity. The absence of *S*-methyltransferase activity in *E. coli* expressing the liverwort Mdd-like gene may have been due to the protein product not folding correctly and/or a lack of appropriate co-factors for activity in this heterologous host. Alternatively, these algal proteins may not constitute genuine Mdd enzymes, despite them containing the same methyltransferase family Pfam domain seen in MddH and MddM1. The function of these Mdd-like proteins remains unknown, requires further investigation and again highlights the importance of substantiating genomic predictions with functional analysis.

2.4 Characterization of recombinant MddM1 and MddM2

Since *M. poriferae* ZYF656 MddM2 proved problematic to purify, the functionally verified ^{Tb}MddM2 from *Thermobispora bispora* was selected for further analysis. Recombinant GST-tagged MddM1 and ^{Tb}MddM2 proteins were overexpressed in *E. coli* BL21 (DE3), and proteins of the expected molecular weight were purified (Figure S5A,B, Supporting information). Both proteins exhibited *in vitro* SAM-dependent *S*-methylation activity with either H_2S or MeSH to yield DMS. The optimal pH and temperature for MeSH *S*-methylation was 9.0 for MddM1 (**Figure 3A**) and 40°C (Figure 3B), respectively, whilst its optimal pH and temperature for H_2S was 7.6 (Figure 3A) and 30°C (Figure 3B), respectively. ^{Tb}MddM2 showed an optimum pH of 8.0 (**Figure 4A**) and temperature of 30°C for both substrates (Figure 4B). Notably, MddM1 and ^{Tb}MddM2 showed no *S*-methylation activity towards most other tested sulfur compounds including Coenzyme A (CoA), cysteine (L-Cys), glutathione (GSH), 2-mercaptoethanesulfonate (Coenzyme M) or the DMSP synthesis intermediates Met and

4-methylthio-2-hydroxybutyrate (MTHB) (Figure S5C,D, Supporting information). Thiols, like ethanethiol and 1-propanethiol, could also serve as the substrates of MddM1 and ^{Tb}MddM2, as was previously shown for MddH (Figure S5C,D, Supporting information).[15]

Enzyme kinetics studies showed MddM1 to have a ~1.6-fold higher K_m value for MeSH (0.76 mM) than for H_2S (0.46 mM), and k_{cat} values that were ~5-fold higher for MeSH (0.21 s^{-1}) (Figure 3C,E). Therefore, MddM1 was ~3-fold more efficient at *S*-methylating MeSH (k_{cat}/K_m: 274.33 M^{-1} s^{-1}) than H_2S (k_{cat}/K_m: 90.30 M^{-1} s^{-1}), indicating a higher consumption rate of MeSH over its production rate in *vitro*. ^{Tb}MddM2 exhibited comparable K_m values for H_2S (0.16 mM) and MeSH (0.22 mM), which were considerably lower than for MddM1 (Figure 4C,E). Conversely, the k_{cat} values for ^{Tb}MddM2 were ~ 3-fold higher for MeSH than H_2S (Figure 4). Thus, ^{Tb}MddM2 also demonstrated greater efficiency in *S*-methylating MeSH (k_{cat}/K_m ~272.73 M^{-1} s^{-1}) than H_2S (k_{cat}/K_m ~125.00 M^{-1} s^{-1}). Specific activity data showed MddM1 and ^{Tb}MddM2 exhibited similar activities towards MeSH, which were ~1.5-fold lower than for H_2S, with ^{Tb}MddM2 having slightly higher activity. The MddM1 and ^{Tb}MddM2 specific activities were substantially higher than for MddA,[14] but lower than MddH.[15]

2.5 Potential roles of MddM1 and MddM2 enzymes

Previous studies implied that the Mdd-driven conversion of toxic H_2S and MeSH to non-toxic DMS may be a cellular strategy for detoxifying these gases and had shown *mddA* and *mddH* transcription to be enhanced by H_2S and/or MeSH.[14-15] Here, *M. poriferae* ZYF656 *mddM1* and *mddM2* transcription was also significantly enhanced by the addition of Met, MeSH and H_2S. Induction by Met implied that the bacterial Mdd pathways can efficiently remove excess MeSH released from Met via Met-gamma-lyase enzymes when this amino acid is in excess. Note, transcriptional induction was always more prominent for *mddM2* (Figure 1E). Interestingly, *mddM1* and *mddM2* transcription was also enhanced by addition of H_2O_2 to mimic oxidative stress (Figure S6, Supporting information), something not previously linked to H_2S and

MeSH *S*-methylation.

The growth of *E. coli* expressing *mddM1* or *mddM2* was examined under stress conditions to study the role of these genes. MddM1 or MddM2 expression in *E. coli* enhanced growth in the presence of H_2S, MeSH and H_2O_2 (**Figure 5**), imping these methyltransferases can play a role in detoxification of H_2S and MeSH, and in oxidative stress protection. For protection against oxidative stress, we hypothesized that DMS might be produced as a source of the antioxidant DMSO,[34] as *M. poriferae* ZYF656 contained the trimethylamine monooxygenase gene *tmm*, whose product can oxidize DMS to DMSO.[35] Furthermore, *M. poriferae* ZYF656 was able to oxidise DMS, potentially generated from H_2S and MeSH, to DMSO (7.91 pmol mg^{-1} protein min^{-1}). This strain was not able to utilize DMSO, DMSP, DMSO, MeSH or Met as a sole carbon or sulfur source supporting the role for DMS production in detoxification and/or oxidative stress tolerance and not assimilation.

2.6 The significance of Mdd systems in diverse environments

To infer the environmental importance of *mddM1*, *mddM2*, *mddA, mddH* and *dddP*, we assessed their relative gene abundance in diverse environmental multi-omics data. Focusing initially on Mariana Trench sediments, where H_2S and MeSH *S*-methylation was proposed to be important,[27] *mddM1* was detected at all depths within sediments from the Trench floor, but no *mddM2* homologues were identified (**Figure 6A**). The proportion of bacteria with *mddM1* homologues remained relatively stable throughout the gravity column core (1.78%-3.80%), with a peak at 78-81 cm (3.80%). *mddM1* was markedly less abundant than *mddA*, the major detected gene in this depth profile, but comparable to *mddH*, except at depths of 10-12 cm and 12-15 cm (Figure 6A). Surprisingly, the most abundant DMSP lyase gene, *dddP*, was predicted to be present in 0.26%-6.07% of bacteria in the Mariana Trench sediments, which was lower than for *mddM1* except in the two samples at 10-12 cm and 12-15 cm (Figure 6A). These data implied that MddM1 and more prominently other Mdd enzymes may play a more important role in DMS production compared to DMSP lyase pathways in Mariana

Trench marine sediments.

Analysis of metagenomes from other diverse environments showed *mddM1* was present in all, but was most abundant in soils (3.30%, Figure 6B), supporting the prediction of H_2S- and MeSH-dependent DMS production being an important process in sedimentary environments.[12, 26, 36] *mddM1* was predicted in 0.02-0.58% marine bacteria, but its prevalence decreased with increasing seawater depth (Figure 6B). In contrast, the relative abundance of *mddM2* was particularly low in all environments (0-0.58%) and no *mddM2* genes were detected in marine water samples (≤ 200 m), cold spring or hydrothermal vents within this dataset (Figure 6B). Cumulatively, the DMSP lyase enzyme DddP was far more abundant than all *mdd* genes in most aquatic samples, but not sediments, implying that DMSP cleavage is the predominant aquatic DMS source (Figure 6B). Moreover, *mddH* also exhibited a wide distribution in various environments (Figure 6B). The taxonomy of prokaryotic *mdd* genes beyond the *Terrabacteria* group and *Proteobacteria* in many metagenomic samples remained challenging. It was worth noting that most MAGs with *mddM1* homologues were annotated as *Actinomycetota*, and 100% of MAGs with *mddM2* homologues were also annotated as *Actinomycetota*, corroborating our above findings that the MddM1 and MddM2 enzymes are primarily in *Actinomycetota*. In Tara Oceans samples from the OM-RGC marine metagenome database, only two *mddM1* homologous genes were detected at extremely low abundance and exhibited a sparse distribution.[37] This low level detection of *mddM1* could be due to these actinomycetes being filamentous and filtered out of Tara Oceans samples; or their preference to colonize marine sediments rather than seawater and OM-RGC database comprising largely pelagic samples.

3 Discussion

The important gas DMS can be biologically produced from many precursor molecules including H_2S, MeSH and DMSO, but DMSP was thought to be the major source. Here, we further highlight the potential importance of H_2S and MeSH dependent DMS production via the discovery and characterization of two novel Mdd enzymes, termed

MddM1 and MddM2. MddM1 was exceptionally common in *Actinomycetota* and in terrestrial and marine sediment environments, the latter being known hotspots for DMS production.[7]

MddM1 and MddM2 encoded SAM-dependent H_2S and MeSH methyltransferases which were both taxonomically distinct to the previously identified MddA, MddH and eukaryotic thiol methyltransferases (Figure 2; S2, Supporting information).[14-15, 26] Despite their taxonomic disparity, MddM1, MddM2, MddH and human TMT1A and TMT1B all shared extended residue similarity, the same conserved SAM-binding domain and significant structural similarity (Figure 2; S2, Supporting information). These data implied that these five *S*-methyltransferase enzymes may share a common ancestor. In contrast, MddA bore no substantial sequence nor structural similarity to MddM2, MddH, TMT1A or TMT1B, implying that it evolved independently. Nevertheless, this study highlighted significant biodiversity in the Mdd enzyme family, which was reminiscent of that observed with DMSP lyases.[10, 15, 38] These data lend further weight to the hypothesis that the enzymatic evolution of H_2S and MeSH *S*-methyltransferase and DMSP cleavage activities were far easier than for DMSP demethylation for example.[10, 15, 38]

Met, H_2S, MeSH and, likely, MMPA are known to be toxic to cells by inhibiting the mitochondrial electron transport chain.[39] These substances can be converted into the harmless gas DMS through a combination of microbial Met-gamma-lyase, downstream DMSP demethylation enzymes and ultimately Mdd-family *S*-methyltransferases.[14-15] Our data reinforces the hypothesis that microbes with an Mdd enzyme, *S*-methylate H_2S and MeSH (potentially from MMPA and/or Met degradation) to produce DMS as a cellular detoxification strategy. In addition, oxidative stress is a continuous factor that bacteria must cope with and a key mechanism associated with MeSH-induced cellular damage.[40] Here, we provide the first evidence for Mdd pathways protecting against oxidative stress through the host upregulating *mdd* genes in response to oxidative stress (from H_2O_2 addition), and the action Mdd proteins in its amelioration. Note, cells have many methods to deal with oxidative stress, e.g. superoxide dismutase and catalase

production, but the specific antioxidant mechanisms of Mdd enzymes remain unknown. It was interesting that there were both membrane-associated (MddA and MddM2) and cyctosolic Mdd (MddH and MddM1) enzymes, perhaps implying extracellular or intracellular sources of the toxic Mdd substrates. A membranous system might better detoxify exterior molecules and vice versa for the cellular generated substrates.

Based on identification of Mdd-like proteins in the MMETSP database and the subsequent finding that one candidate algal Mdd enzyme lacked *S*-methyltransferase activity against the canonical substrates, it was possible that these proteins comprise a clade of Mdd-like methyltransferase enzymes which evolved to methylate a substrate distinct from H_2S or MeSH, and not necessarily related to sulfur cycling. As noted above, it is also possible that the chosen candidate algal Mdd-like protein did not properly fold when expressed in *E. coli* or that it required a missing co-factor for activity. Further studies are required on more representative proteins from this diverse clade to draw robust conclusions on their role and environmental importance. Nevertheless, this finding highlights the critical importance of coupling genomic predictions with functional analyses and of the necessity of comprehensively considering potential substrate range.

The significance of the Mdd pathways in global DMS production, with far-reaching implications for atmospheric chemistry, climate, and sulfur cycling, has been underestimated in the past. Here, we showed that the genetic potential for DMS production via Mdd systems could be more prominent in the terrestrial and marine sediments than DMSP-dependent systems, including those of the deep ocean where *M. poriferae* ZYF656, the source of MddM1 and MddM2, was isolated. It is likely that Met, MeSH and H_2S are more prominent in microoxic-anoxic sediments than in seawater, perhaps explaining the abundance of *mdd* genes, particularly from *Actinomycetota*, in these environments. This study builds on previous identification of Mdd systems to further highlight the growing potential importance of Mdd and DMSP systems to global DMS production in both marine and terrestrial settings.

There is a pressing need for more environmental measurements of MeSH, H_2S, DMSP

and other potential DMS sources, with DMSP- and Mdd-dependent DMS production rates and multi-omics (ideally metatranscriptomics and metaproteomics) to allow a better understanding of the relative importance of the microbes and pathways that generate DMS in diverse environments. Without such comprehensive studies it is very difficult to estimate the exact contribution of Mdd pathways, or any other pathway, to the global DMS production. Nevertheless, this study emphasizes that Mdd systems cannot automatically be ignored as insignificant contributors to global DMS production and introduces the *Actinomycetota* as potentially important contributors in diverse environments.

4 Conclusions

This study identified two novel SAM-dependent methyltransferases, MddM1 and MddM2, predominantly found in diverse marine and terrestrial actinomycetes, many of which were not previously thought to *S*-methylate H_2S and MeSH. Thus, it highlighted the large biodiversity in Mdd enzymes, with four distinct known Mdd enzymes, and implied that Mdd enzymes, like DMSP lyases, evolved multiple times. We confirmed the important role of Mdd proteins to detoxify cytotoxic H_2S and MeSH through their *S*-methylation yielding DMS, but also, for the first time, oxidative stress amelioration. Given over 50% of *Actinomycetota* contain *mddM1* and the abundance of *mdd* genes in diverse soils and marsh sediments, this study implicates H_2S/MeSH-dependent *S*-methylation as a major and previously underestimated contributor to global DMS production and sulfur cycling. Future research must combine detailed multiomics studies with measurements of Mdd pathways and other DMS production and consumption processes to further elucidate the relative importance of these pathways in diverse marine and terrestrial environments.

5 Experimental Section

Bacterial strains, plasmids, and culture media. Strains and plasmids used in this study are listed in Table S2 (Supporting information). *M. poriferae* ZYF656 was grown

in 2216E complete medium (per liter seawater: 1 g yeast extract, 5 g peptone, 0.01 g ferric phosphate, 20 g agar, pH 7.6) or MBM minimal medium with a mixed carbon source[41] at 28°C, 170 r.p.m. for 24 h. *Escherichia coli* was cultured in LB complete medium or M9 minimal medium at 37°C overnight. The composition of the M9 minimal medium was as follows (per 200 mL water): 40 mL 5 × M9 salt (per liter water: 64 g $Na_2HPO_4·7H_2O$, 15 g KH_2PO_4 and 2.5 g NaCl), 200 μL 0.1M $CaCl_2$, 400 μL 1M $MgSO_4$, 200 μL 30 mg/mL Thiamine and 360 μL 50% glycerol. *S. venezuelae* wild-type and mutant strains were cultured in MYM complete medium (per liter water: 4 g maltose, 4 g yeast extract, 10 g malt extract, 18 g agar, pH 7.3) or MM minimal medium (per liter water: 0.5 g *L*-asparagine, 0.5 g K_2HPO_4, 0.2 g $MgSO_4·7H_2O$, 0.01g $FeSO_4·7H_2O$, 10 g glucose, 10 g agar, pH to 7.0-7.2) at 28°C, 170 r.p.m. for 48 h. Throughout this study, 'water' refers to purified, deionized water used consistently for all media preparations. When required for selection, antibiotics were added at the following concentrations: ampicillin (50 μg/mL), chloramphenicol (25 μg/mL), kanamycin (50 μg/mL).

Isolation of *M. poriferae* ZYF656. *M. poriferae* ZYF656 was isolated from 9,600 m depth seawater of the Challenger Deep of the Mariana Trench (11°20.605′N, 142°19.557′E), aboard the R/V *Dong Fang Hong 2* on September, 2016. For the isolation of bacteria, seawater sample (1 mL) was diluted in gradient and spread on 2216E on board. All plates were incubated at 28°C for 5-7 days. Most colonies were picked, purified for three times and preserved at -80°C with glycerol (15%, v/v). The bacterial genomic DNA was extracted, and then amplified with the universal primers 27F/1492R for bacterial identification (Table S3, Supporting information). One isolate ZYF656, identified as *M. poriferae*, attracted our attention as it showed Mdd activity, but lacked all known *mdd* genes.

Sole carbon or sulfur source growth tests. *M. poriferae* ZYF656 cells were harvested, washed with MBM medium three times and used to inoculate fresh MBM medium

lacking a carbon or sulfur source. Met (Sigma Aldrich, USA; 5 mM), DMSP (TCI, Shanghai, China; 5 mM), DMSO (Solarbio, Beijing, China; 2 mM), DMS (Sigma Aldrich, USA; 1 mM), glycerol (Sinopharm, Shanghai, China; 10 mM), MeSH (Sigma Aldrich, USA; 1 mM), glucose (Sinopharm, Shanghai, China; 2 mM), sucrose (Sinopharm, Shanghai, China; 2 mM), sodium succinate (Sigma Aldrich, USA; 2 mM) or sodium pyruvate (Yuanye Bio-Technology Co., Ltd, Shanghai, China; 2 mM) were added as the sole carbon. Where necessary, Met, DMSP, DMSO, DMS, MeSH, or $MgSO_4$ (100 μM, respectively) were added as the sole sulfur source. Cultures were incubated at 28°C, 170 r.p.m. for 10 days, and cell growth was followed by measuring optical density at 600 nm (OD_{600}) using a WFJ 2100 spectrophotometer (Unico, Shanghai, China).

Analysis of microbial DMS and MeSH production. *M. poriferae* ZYF656 Colonies from fresh agar plates were picked and used to inoculate MBM medium (200 μL) containing Met (0.5 mM), MMPA (Tokyo Chemical Industry Co., Ltd., Tokyo, Japan; 0.5 mM), or MeSH (0.5 mM) in a 2 mL vial, which were incubated at 28℃, 170 r.p.m. for 24 h. To measure DMS and MeSH production from H_2S, strains were inoculated into 2216E medium without Fe^{3+} and incubated with H_2S (0.5 mM) at 28°C for a further 24 h. The *S. venezuelae* wild-type and its series of knockout, complemented, and overexpressing strains colonies from fresh MYM agar plates were inoculated into solid slants of MM medium (300 μL) containing the addition of Met (1 mM) or MeSH (1 mM) in 2 mL sealed GC vials and incubated at 28℃ for 48 h. The production of MeSH and DMS was expressed in μmol and nmol, respectively. All experiments were performed with three biological replicates.

Headspace DMS and MeSH levels were directly monitored by gas chromatography (GC) using a flame photometric detector (Agilent 7890A GC fitted with a 7693 autosampler) and a HP-INNOWax 30 m × 0.320 mm capillary column (Agilent Technologies, J&W Scientific). Culture medium with and without substrate were used as negative controls. Calibration curves were generated as previously described.[42] The

476 detection limit for DMS and MeSH was 0.2 nmol and 5 nmol, respectively. Bacterial
477 cells were lysed by ultrasonication (JY92 IIN, Scientz, Ningbo, China) and total protein
478 was quantified by Bradford assays (BioRad, Hemel Hempstead, UK). Experiments
479 were conducted in triplicates and quantitative results were shown as mean ± s.d.
480
481 **Analysis of microbial DMSO production.** *M. poriferae* ZYF656 colonies from fresh
482 agar plates were picked and inoculated into MBM medium (200 µL) containing DMS
483 (1 mM) in 2 mL sealed vials and incubated at 28°C, 170 r.p.m. for 24 h. All traces of
484 DMS were eliminated by opening the lid and heating the reaction vials in an 85°C water
485 bath for 2 h. Subsequently, vials were sealed immediately after the addition of stannous
486 chloride (100 µL; 880 mM, 16.68 g in 100 mL of 37% HCl), and heated at 55°C for 90
487 min. DMS was quantified by gas chromatography, as described above.
488
489 **Genome sequencing of *M. poriferae* ZYF656.** *M. poriferae* ZYF656 colonies were
490 provided to the Beijing Genomics institution (BGI; Wuhan, China) who collected
491 performed genomic DNA sequencing. Whole genome sequencing was done using the
492 Illumina Hiseq 4000 sequencer system with a 270 bp paired-end library and PacBio
493 RSII and a 20 kb library. Reads were assembled using Unicycle, sequencing data
494 correction was performed with Pilon v1.1, and artificial correction of ambiguous sites
495 was carried out with REAPR 1.0. Genome annotation was performed by the RASTtk
496 online service with default settings applied.[43] Ratified enzymes involved in DMSP/S
497 cycling, shown in Table S4 (Supporting information), were used as query sequences for
498 BLASTp.
499
500 **Construction of *M. poriferae* ZYF656 genomic library.** A genomic library of *M.*
501 *poriferae* ZYF656 was constructed to identify novel Mdd enzymes. High quality *M.*
502 *poriferae* ZYF656 genomic DNA was partially digested with the restriction
503 endonuclease *Bam*HI, and ligated into *Bam*HI-digested and dephosphorylated plasmid
504 pUC18. Ligated mixes were transformed into *E. coli* JM109 to form a library with

approximately 10,000 clones, from which eight clones were randomly selected to determine the library quality and coverage. The eight chosen plasmids were analysed by restriction digestion with *Bam*HI, and all had 20-30 kbp of cloned DNA with distinct restriction digestion profiles and cloned sequences. To screen for clones conferring MeSH-dependnet DMS production, *E. coli* JM109 transformants were cultured in LB medium with ampicillin (50 μg/mL) at 28℃, 170 r.p.m. for 12-14 h, and diluted 1/50 into M9 medium containing MeSH (1 mM) and ampicillin (50 μg/mL). The strains were cultured at 37℃ for 24 h, and screened by GC. *E. coli* JM109 with empty pUC18 vector and media only, with or without MeSH, were used as controls. Positive clones producing DMS above the negative controls were sequenced by Sangon Biotech (Shanghai, China).

General genetic manipulations. The primers used in this study are shown in Table S3 (Supporting information). Bacterial genomic DNA was isolated using a FastPure bacteria DNA isolation mini kit-Box2 (Vazyme, Nanjing, China). Plasmids purification and gel extraction used a E.Z.N.A. plasmid mini kit I and a E.Z.N.A. gel extraction kit (Omega, Georgia, USA), respectively. Routine restriction digestions and ligations were performed as described in Carrión et al. 2015.[26] Plasmids pXMJ19 with ^{Tb}*mddM2* and *mddM1* were individually transferred to *E. coli* DH5α by transformation. Preparation of competent cells: *C.* RES167 was cultured overnight at 30°C, and subsequently inoculated into BHIS medium (per 200 mL water: 7.4 g brain heart infusion and 18.2 g sorbitol) until the OD_{600} reached 1.75. The cells were harvested by centrifugation at 5,000 *g* for 20 min, resuspended in 20 mL precooled TG buffer (per 100 mL water: 1 mM Tris-HCl and 12 g 87% glycerol), and repeated this step twice. The TG buffer was then replaced with precooled glycerol (10%) and the procedure performed twice more. Finally, the cells were resuspended in 10% glycerol (1 mL) and dispensed into aliquots (150 μL) in cooled Eppendorf tubes. Plasmids were transformed into competent *C. glutamicum* RES167 by electroporation as previously described.[44] To measure DMS production from MeSH or H_2S of RES167/pXMJ19-*mddM1* and RES167/pXMJ19-

534 ^{Tb}*mddM2*, these two strains were cultured in 2 mL sealed glass vials into M9 medium
535 (200 μL) supplemented with MeSH (1 mM) or H_2S (1 mM), glucose (2 mM) and
536 chloramphenicol (25 μg/mL) at 30°C for 24h.
537 Full-length *mddM1* from *M. poriferae* ZYF656 and ^{Tb}*mddM2* genes were PCR-
538 amplified from genomic DNA and individually cloned into the pGEX-4T-1 vector
539 (Miaoling Biology, Wuhan, China) for expression of GST-tagged enzymes in *E. coli*
540 BL21 (DE3). Sequencing of all PCR-amplified products and plasmids was confirmed
541 by Sangon Biotech Co., Ltd.
542
543 **Protein bioinformatics and localization.** The physical and chemical properties of
544 MddM1 and MddM2 were predicted using protParam
545 (https://web.expasy.org/protparam/).[45] CELLO v 2.5 (http://cello.life.nctu.edu.tw/)
546 was used to predict Mdd protein subcellular localization.[46] The presence of signal
547 peptides in proteins and their cleavage sites were predicted through the SignalP 5.0
548 server (https://services.healthtech,dtu.dk/service/SignalP-5.0).[47] The transmembrane
549 helices in proteins were predicted by TMHMM-2.0
550 (https://services.healthtech,dtu.dk/service/TMHMM-2.0).[48] The membrane and
551 cytoplasmic proteins of *M. poriferae* ZYF656 were extracted using the Bacterial
552 Membrane Protein/Cytoplasmic Protein Extraction kit (Solarbio, Beijing, China) in
553 accordance with the manufacturer's instructions, yielding membrane proteins
554 (400.0 mg/mL) and cytoplasmic proteins (11.0 mg/mL). Given that *M. porifera*
555 ZYF656 is a Gram-positive bacterium, the cell lysis process was extended appropriately,
556 typically for 2 to 4 hours. Subsequently, membrane proteins (10.0 mg) and cytoplasmic
557 proteins (1.2 mg) were each resuspended in Tris-HCl (pH 8.0) with MeSH (1 mM) and
558 SAM (1 mM) to a final volume (150 μL), and incubated at 37°C for 3 h. DMS
559 production was quantified as described above.
560
561 **Protein expression and purification.** Recombinant strains containing pGEX-4T-1
562 were cultured at 37°C overnight with shaking at 170 r.p.m. in LB medium (5 mL) with

ampicillin (50 μg/mL) for positive selection. Afterwards, the cultures were inoculated into fresh LB medium and cultivated until OD_{600} reached 0.5. Isopropyl-D-thiogalactopyranoside (IPTG) was added to cultures at a final concentration (0.1 mM), which were then further incubated at 16℃ for 14-16 h. Cells were harvested, washed and resuspended in PBS buffer (140 mM NaCl, 2.7 mM KCl, 10 mM Na_2HPO_4, 1.8 mM KH_2PO_4, pH 7.3), lysed by sonication using an ultrasonic homogenizer JY92 IIN (Scientz, Ningbo, China), and then centrifugated at 12,000 *g* for 10 min. Protein was purified from cell supernatant by Glutathione Sepharose 4B affinity chromatography (GE Healthcare, USA), and the bound proteins were eluted in the elution buffer (50 mM Tris-HCl, 10 mM reduced glutathione, pH 8.0). Purified proteins were analyzed by SDS-PAGE, and stored at -80℃.

To determine the functionality of MddM1 and MddM2 homologues, candidate MddM1 homologous proteins sequences from *Streptomyces* sp. SAJ15 (A0A7M3LRJ1), *Planomonospora sphaerica* (A0A161LM11), *Acidobacteriota_bacterium* (MCZ6599416.1), *Acidobacteriota_bacterium* (MDE3069982.1), *Mycolicibacterium_litorale* (A0A6S6P9F0), *Deltaproteobacteria_bacterium* (TMB00698.1), *Dictyobacter_kobayashii* (WP_126557608.1), *Streptomyces_venezuelae* (F2RA35) and the MddM2 homologous protein sequence from *T. bispora* (D6Y5L2) were obtained from UniproKB (Table S5, Supporting information), and synthesized by Sangon Biotech (Shanghai, China). They were subcloned into pET-24a, and transformed into *E. coli* BL21 (DE3). The recombinant strains were grown in LB with kanamycin (50 μg/mL) to an OD_{600} of 0.5, and then cultured with IPTG (0.1 mM) at 28℃, 170 r.p.m. for 3 h. Cells containing overexpressed protein were collected and sonicated as described above. Triplicate sonicated mixture (200 μL) of the supernatants and pellets were incubated with SAM (1 mM) and MeSH (1 mM) or H_2S (1 mM) for 3 h before quantifying the MeSH and DMS levels and protein concentrations.

***In vitro* characterization of Mdd enzymes.** The enzymatic activity of MddM1 and ^{Tb}MddM2 were measured by detecting MeSH and DMS production as previously described.[14] Reaction mixtures (200 μL) containing Tris-HCl (20 mM, pH9.0), purified protein (1 μg MddM1 or 2 μg ^{Tb}MddM2), SAM (1 mM) and MeSH (1 mM) or H_2S (1 mM) were incubated at 28℃ for 30 min, and stopped by adding HCl (100 μL, 10%). The MeSH and/or DMS produced was monitored by GC. Enzyme-deficient reaction mixtures provided negative controls to ensure abiotic DMS formation was absent. To determine the optimal temperature, reaction mixtures were incubated at 4 to 60℃ for 30 min. The optimum pH was conducted at the optimal temperature, and Tris-HCl was replaced with Britton-Robinson buffer (Boric acid, phosphoric acid and acetic acid, pH adjusted with NaOH) at pH values of 4 to 10.6. For kinetic parameter assays, K_m and k_{cat} values were determined by nonlinear regression analysis using purified proteins (1 μg MddM1 or 2 μg ^{Tb}MddM2) and SAM (0-2.0 mM, fixed at 1 mM for MeSH kinetic work), MeSH or H_2S (0-2.0 mM, fixed at 1 mM for SAM kinetic work). The enzymatic activities were also examined under the optimum temperature and pH, and quenched by addition of HCl (100 μL, 10%). Enzyme activity was calculated by the amount of DMS production when using MeSH as substrate, and by the sum of MeSH and twice DMS production when using H_2S as substrate. Non-linear fitting of the data was performed by the Graphpad Prism8.

LC-MS analysis. LC-MS was used to confirm the conversion of SAM to *S*-adenosyl-homocysteine (SAH) in enzyme assays with purified protein to verify substrate specificity. LC-MS was carried out on a QTRAP4500 liquid chromatograph mass spectrometer (SCIEX, Netherlands) with a SunFire C18 reversed-phase column (4.6 × 250 mm, 5 μm particle size, Waters, United States). The MS spray chamber conditions were as follows: curtain gas 35 psi, ion spray voltage 5,000 V, ion spray temperature 450℃, ion source gas1 40 psi, ion source gas1 45 psi, collision gas medium. Solvent A was ammonium acetate (50 mM, pH 5.5). Solvent B was 20% acetonitrile and 80% solvent A. The samples were eluted with a linear gradient of 95% solvent A to 95%

solvent B over 16 min at the flow of 0.8 mL/min. Prior to use, the solvent was subjected to ultrasonic shock for 20 mins to remove dissolved gases. The injection volume was 10 μL. All samples were centrifuged at 12,000 *g* for 15 min, after which, each sample (100 μL) was transferred to 2 mL glass vials equipped with internal cannulas. The targeted mass transitions corresponding to $[M+H]^+$ of SAH and SAM were detected as previously described.[49-50]

Determination of MddM1 and MddM2 activity in *E. coli*. *E. coli* BL21 strains containing cloned *mddM1* and *mddM2* genes or empty vector were cultured in LB medium (5 mL) containing ampicillin (50 μg/mL) until an OD_{600} of 0.8 was reached. The cells were diluted 10-fold into M9 minimal medium (300 μL) with IPTG (0.1 mM) and MeSH (0.5 mM) or H_2S (0.5 mM), and incubated at 28℃ for 18 h.[26] DMS production, MeSH production and protein concentrations were determined as above.

Construction of *Streptomyces venezuelae* mutants

A mutation of *mddM1* (*S. venezuelae* Δ*mddM1*) was constructed in *S. venezuelae* (GenBank accession number: NZ_CP018074.1). gRNA sequences to the target region were ordered as single stranded oligos with *Bbs* I overhangs from Integrated DNA technologies (IDT) and annealed at equal molarity in HEPES buffer by heating at 95℃ for 5 min before cooling to 4℃ (at 1℃/s). To assemble into the pCRISPomyces-2 vector, Golden Gate reactions were set up using purified backbone (100 ng) and insert (3μL) in the presence of T4 ligase buffer (2 μL), T4 ligase (1 μL), *Bbs* I (1 μL) and dH_2O up to total volume (20 μL). Around 1 kbp of flanking DNA from either side of the target gene was PCR amplified using Q5 DNA polymerase.

pCRISPomyces-2 containing the gRNA of interest was digested with *Xba* I and dephosphorylated with shrimp alkaline phosphatase to prevent re-ligation. Flanking DNAs were assembled into the digested vector backbones containing the gRNAs using Gibson Assembly. DNAs were incubated in a ratio of 1:3 (plasmid/insert) in the presence of Gibson Assembly master mix (NEB) at 50℃ for 1 h. The resulting reaction

mix was then transformed into *E. coli* and plated on selective media at 37°C overnight and the resulting colonies were screened by colony PCR.

Confirmed plasmids were transformed into *E. coli* ET12567 containing pUZ8002. These were then grown overnight at 37°C, 200 r.p.m., sub-cultured 1:20 in fresh LB + relevant antibiotics and grown to OD_{600} 0.4 - 0.6. Pellets from culture (10 mL) were washed twice with fresh LB to remove antibiotics. Meanwhile, *S. venezuelae* spores (200 µL) were pre-germinated in 2×YT (500 µL; per litre water: 16 g tryptone, 10 g yeast extract, 5 g NaCl, pH 7.0) at 52°C for 10 minutes. The two cell types were mixed, resuspended in fresh LB and plated onto SFM medium (per litre water: 20 g soy flour, 20 g mannitol, 20 g agar) containing $MgCl_2$ (10 mM) and incubated at room temperature for 16 h. For selection of desired ex-conjugants, Nalidixic acid (0.5 mg) and selection antibiotic was added in dH_2O (1 mL) to each plate and cultures returned to the 30°C incubator for 2-3 days or until colonies appeared.

For overexpression, pIJ10257 containing the constitutive *ErmE** promoter, was digested with *Nde* I and *Hin*d III and gel purified as described above. The gene of interest was PCR amplified using Q5 Polymerase and plasmids were assembled using Gibson assembly. Confirmed plasmids were transformed into *E. coli* ET12567 containing pUZ8002 for conjugation into both wild-type *S. venezuelae* or its *mddM1* mutant. Resulting exconjugants were confirmed to contain the overexpression plasmid by antibiotic selection and colony PCR using Biotaq red. All *Streptomyces* strains were routinely grown on MYM medium at 30°C for 3 days until the green spore pigment was visible indicating a complete life cycle. The plasmids and primers used are listed in Tables S2 and S3 (Supporting information).

Growth analyses of *E. coli* with *mddM1* and *mddM2* genes. *E. coli* BL21 strain containing *mddM1* gene, *mddM2* gene or empty vector was cultured in LB medium (5mL) at 37°C overnight and the OD_{600} was adjusted to 0.5. The cells were then diluted 10-fold into fresh M9 minimal medium with MeSH (1 mM), H_2S (1 mM) or H_2O_2 (2 mM) and ampicillin (50 µg/mL) in a 96-well microplate, and incubated at 37°C.[14] The

absorbance of the bacterial suspensions was measured at 600 nm using a Multiskan GO microplate reader (Thermo scientific, USA). An equal amount of distilled water was added to the bacterial suspensions instead of MeSH, H_2S or H_2O_2 as the negative control.

RT-qPCR analysis. *M. poriferae* ZYF656 was cultured in 2216E medium at 28℃ until logarithmic growth phase was reached. Cells were diluted 10-fold into fresh MBM minimal medium containing Met (1 mM), H_2S (1 mM) or MeSH (1 mM) and incubated at 28℃, 170 r.p.m. for 8 h. Cells cultured in MBM medium without substrate were used as controls. Each sample was performed in triplicate, and collected by centrifugation at 5,000 *g* for 10 min. Total RNA was extracted using a RNeasy Mini kit (Qiagen, Germary), and reverse transcribed using a NZY First-Strand cDNA Synthesis kit (Nzytech, China). Fluorescence quantitative PCR was performed using a QuantStudio™ 5 System (Thermo Fisher Scientific, USA). Data were analyzed by the $2^{-\triangle\triangle CT}$ method, and *recA* was used as an internal standard. Forward and reverse primer pairs were designed as shown in Table S3 (Supporting information).

Bioinformatics analysis. BLASTp was used to identify candidate MddM1 and MddM2 homologues (identity ≥ 40%, E-value ≤ e-30, and coverage ≥ 70%) in the Uniprot (https://www.uniprot.org/) and NCBI NR (https://www.ncbi.nlm.nih.gov/) databases.[51] MddM1 and MddM2 of *M. poriferae* ZYF656 were used as the query sequences, respectively. The phylogenetic tree was constructed at IQ-TREE website (http://iqtree.cibiv.univie.ac.at/). The information for representative MddM proteins is shown in Table S6 (Supporting information). The amino acid sequences were aligned using MAFFT (https://mafft.cbrc.jp/alignment/server/) and uploaded to the Gblocks website (http://molevol.cmima.csic.es/castresana/Gblocks server) for gap removal. The maximum-likelihood method and the LG+F+G4 model of amino acid substitution were used with 1,000 bootstrap replications. The tree was visualized by Chiplot.[52] MddM1 homologous proteins shown in Table S4 (Supporting information) from distinct branches or bacterial clades were selected to further study to verify their Mdd activities.

To explore the distribution of MddM1, MddM2, MddA and MddH across the *Actinomycetota*, ratified protein sequences of MddM1, MddM2, MddA and MddH were used as query sequences to perform Hidden Markov Model (HMM)-based searches (E-value ≤ e-55) from all representative genomes of *Actinomycetota* from NCBI (42,815 in total) using HMMER (v3.4) (https://github.com/EddyRivasLab/hmmer.git), BLASTp searches against peptide databases from the genomes obtained in the previous step, and set the alignment threshold to identity ≥ 40% and coverage ≥ 70%. Metagenomes containing actinomycetes with at least 5% abundance were screened from the Sandpiper 0.2.0 (http://sandpiper.qut.edu.au), and the biogeographic distribution of the actinomycetes was plotted by R (v. 4.0.3) using scatterpie and ggplot2.

To analyze the distribution of MddM1, MddM2, MddA, MddH and DddP in different environmental metagenomes, we downloaded environmental metagenomes using the online webserver from the Integrated Microbial Genomes & Microbiomes (IMG/M) system[53] and NCBI SRA database,[54] and the genome information are shown in Table S7 (Supporting information). Metagenomic sequencing and binning were performed as previously described.[27] The MddM1, MddM2, MddA, MddH and DddP sequences used for the metagenome analysis are detailed in Table S4 (Supporting information). RecA sequences were extracted from Cheng et al. 2023.[27] HMM-based searches (E-value ≤ e-55) for Mdd homologues in metagenomes from different environments using cutoff values of identity ≥ 40%, E-value ≤ e-55, and coverage ≥ 70% were retrieved by BLASTp. The abundance of *mdd* genes was calculated using the percentages of bacterial harboring genes normalized to the single-copy housekeeping gene *recA*.

For Eukaryotes, homologues of MddM1, MddM2 and MddH were identified from re-assemblies of the Marine Microbial Eukaryote Transcriptome Sequencing Project (MMETSP) (https://doi.org/10.5281/zenodo.740440) using HMM searches with an E-value of 1×10^{-30} for MddM1 and MddM2, and 1×10^{-80} for MddH.[33] The obtained sequences were further refined with identity ≥ 35% and coverage ≥ 70%. The maximum-likelihood tree of eukaryotic Mdd homologues was constructed using IQ-

TREE. The resulting tree was visualized in Itol.[55]

Acknowledgements

This work was funded by the National Natural Science Foundation of China (32370118, 42306115 and 42376101), National Key R&D Program of China (2025YFF0516900 and 2025YFF0516903), Shandong Provincial Natural Science Foundation (ZR2023QD017), China Postdoctoral Science Foundation (2022M722975), the Postdoctoral Innovation Program of Shandong Province (SDCX-ZG-202201016), the Biotechnology and Biological Sciences Research Council, UK (BB/X005968), Natural Environmental Research Council, UK (NE/P012671) and China Scholarship Council (No. 202106330012).

Conflict of Interest

The authors declare no conflict of interest.

Author Contributions

X.-H.Z. and J.D.T. were responsible for the conceptualization of the study. Experiments were carried out by R.H.G. and Y.Z. (identification and characterization of MddM, genomic library construction and growth experiments), Z.H.G. (H_2S experiments, candidate MddM expression and characterization, mutant strains construction, membrane protein extraction, Y.H.Z. (screening and identification of novel Mdd strains, establishment of Mdd activity experimental method), R.D. (mutant construction), C.S. (phenotypic experiments of the mutant strains) and Y.F.Z. (isolation of bacterial strains). Data analysis was carried out by R.H.G. (genetic taxonomy), Z.H.G. (genome and MMETSP database alignment), H.J.C. (metagenome), R.H.L. (bioinformation) and A.J.G. (enzymatic kinetics). X.-H.Z. and Y.H.Z. were accountable for the supervision of the study. The original draft of the manuscript was written by R.H.G., Z.H.G. and Y.Z. Writing—Review and Editing was also performed by X.-H.Z., J.D.T., R.H.G., Z.H.G., Y.H.Z. and A.J.G.

Data Availability Statement

All data needed to evaluate the conclusions in the paper are present in the paper and/or the Supplementary information.

Received: ((will be filled in by the editorial staff))
Revised: ((will be filled in by the editorial staff))
Published online: ((will be filled in by the editorial staff))

Reference

[1] M. O. Andreae, *Mar. Chem.* **1990**, *30* (1-3), 1, https://doi.org/10.1038/nature1058010.1016/0304-4203(90)90059-L.
[2] J. Stefels, M. Steinke, S. Turner, G. Malin, S. Belviso, *Biogeochemistry* **2007**, *83* (1-3), 245, https://doi.org/10.1007/s10533-007-9091-5.
[3] A. R. J. Curson, J. D. Todd, M. J. Sullivan, A. W. B. Johnston, *Nat. Rev. Microbiol.* **2011**, *9* (12), 849, https://doi.org/10.1038/nrmicro2653.
[4] K. B. Ksionzek, O. J. Lechtenfeld, S. L. McCallister, P. Schmitt-Kopplin, J. K. Geuer, W. Geibert, B. P. Koch, *Science* **2016**, *354* (6311), 456, https://doi.org/10.1126/science.aaf7796.
[5] P. K. Quinn, T. S. Bates, *Nature* **2011**, *480* (7375), 51, https://doi.org/10.1038/nature10580.
[6] S. M. Vallina, R. Simó, *Science* **2007**, *315* (5811), 506, https://doi.org/10.1126/science.1133680.
[7] F. E. Hopkins, S. D. Archer, T. G. Bell, P. Suntharalingam, J. D. Todd, *Nat. Rev. Earth Env.* **2023**, *4* (6), 361, https://doi.org/10.1038/s43017-023-00428-7.
[8] G. A. Nevitt, F. Bonadonna, *Biol. Letters* **2005**, *1* (3), 303, https://doi.org/10.1098/rsbl.2005.0350.
[9] M. Steinke, J. Stefels, E. Stamhuis, *Limnol. Oceanogr.* **2006**, *51* (4), 1925, https://doi.org/10.4319/lo.2006.51.4.1925.
[10] X. H. Zhang, J. Liu, J. Liu, G. Yang, C. X. Xue, A. R. J. Curson, J. D. Todd, *Sci. China Life Sci.* **2019**, *62* (10), 1296, https://doi.org/10.1007/s11427-018-9524-y.
[11] E. G. Stets, M. E. Hines, R. P. Kiene, *FEMS Microbiol. Ecol.* **2004**, *47* (1), 1, https://doi.org/10.1016/S0168-6496(03)00219-8.
[12] O. Carrion, J. Pratscher, A. R. J. Curson, B. T. Williams, W. G. Rostant, J. C. Murrell, J. D. Todd, *ISME J.* **2017**, *11* (10), 2379, https://doi.org/10.1038/ismej.2017.105.
[13] O. Carrion, J. Pratscher, K. Richa, W. G. Rostant, M. Farhan Ul Haque, J. C. Murrell, J. D. Todd, *Front. Microbiol.* **2019**, *10*, 1040, https://doi.org/10.3389/fmicb.2019.01040.
[14] C.-Y. Li, H.-Y. Cao, Q. Wang, O. Carrion, X.-Y. Zhu, J. Miao, P. Wang, X.-L. Chen, J. D. Todd, Y.-Z. Zhang, *ISME J.* **2023**, *17* (8), 1184, https://doi.org/10.1038/s41396-023-01430-z.
[15] Y. Zhang, C. Sun, Z. Guo, L. Liu, X. Zhang, K. Sun, Y. Zheng, A. J. Gates, J. D. Todd, X.-H. Zhang, *Nat. Microbiol.* **2024**, (10), 2614, https://doi.org/10.1038/s41564-024-01788-6.
[16] W. Fei, M. C. Peter, *Environ. Toxicol. Chem.* **1999**, *18*, 2526, https://doi.org/10.1002/etc.5620181120.
[17] Johnson, Beehler, Sakamoto-Arnold, *Science* **1986**, *231* (4742), 1139.

[18] R. P. Kiene, L. J. Linn, *Geochim. Cosmochim. Ac.* **2000**, *64* (16), 2797, https://doi.org/https://doi.org/10.1016/S0016-7037(00)00399-9.
[19] C. R. Reisch, M. A. Moran, W. B. Whitman, *J. Bacteriol.* **2008**, *190* (24), 8018, https://doi.org/10.1128/JB.00770-08.
[20] X. Shao, H.-Y. Cao, F. Zhao, et al., *Mol. Microbiol.* **2019**, *111* (4), 1057, https://doi.org/10.1111/mmi.14211.
[21] Boden, Rich, Borodina, Elena, Wood, P. Ann, Kelly, P. Donovan, Murrell, J. Colin, *J. Bacteriol.* **2011**, *193* (5), https://doi.org/10.1128/JB.00977-10.
[22] E. Borodina, D. P. Kelly, F. A. Rainey, N. L. Ward-Rainey, A. P. Wood, *Arch. Microbiol.* **2000**, *173* (5-6), 425, https://doi.org/10.1007/s002030000165.
[23] R. Bentley, T. G. Chasteen, *Chemosphere* **2004**, *55* (3), 291, https://doi.org/10.1016/j.chemosphere.2003.12.017.
[24] B. J. Maldonato, D. A. Russell, R. A. Totah, *Sci. Rep.* **2021**, *11* (1), 4857, https://doi.org/10.1038/s41598-021-84218-5.
[25] J. M. González Dalmasy, C. M. Fitzsimmons, W. J. E. Frye, et al., *Chem.-Biol. Interact.* **2024**, *394*, 110989, https://doi.org/https://doi.org/10.1016/j.cbi.2024.110989.
[26] O. Carrión, A. R. J. Curson, D. Kumaresan, Y. Fu, A. S. Lang, E. Mercadé, J. D. Todd, *Nat. Commun.* **2015**, *6*, https://doi.org/10.1038/ncomms7579.
[27] H. Cheng, Y. Zhang, Z. Guo, X. He, R. Liu, X.-Y. Zhu, J. Li, J. Liu, X.-H. Zhang, *Appl. Environ. Microb.* **2023**, *89* (7), https://doi.org/10.1128/aem.00251-23.
[28] F. Teufel, J. J. Almagro Armenteros, A. R. Johansen, et al., *Nat. Biotechnol.* **2022**, *40* (7), 1023, https://doi.org/10.1038/s41587-021-01156-3.
[29] J. Abramson, J. Adler, J. Dunger, et al., *Nature* **2024**, *630* (8016), 493, https://doi.org/10.1038/s41586-024-07487-w.
[30] J. Ehrlich, Q. R. Bartz, R. M. Smith, D. A. Joslyn, P. R. Burkholder, *Science* **1947**, *106* (2757), 417, https://doi.org/doi:10.1126/science.106.2757.417.
[31] J. Ehrlich, D. Gottlieb, P. R. Burkholder, L. E. Anderson, T. G. Pridham, *J. Bacteriol.* **1948**, *56* (4), 467, https://doi.org/doi:10.1128/jb.56.4.467-477.1948.
[32] K. S. Hwang, H. U. Kim, P. Charusanti, B. Palsson, S. Y. Lee, *Biotechnol. Adv.* **2014**, *32* (2), 255, https://doi.org/10.1016/j.biotechadv.2013.10.008.
[33] P. J. Keeling, F. Burki, H. M. Wilcox, et al., *PLoS Biol.* **2014**, *12* (6), e1001889, https://doi.org/10.1371/journal.pbio.1001889.
[34] H. L. Cui, *Molecules* **2022**, *27* (23), https://doi.org/10.3390/molecules27238480.
[35] Y. Chen, N. A. Patel, A. Crombie, J. H. Scrivens, J. C. Murrell, *Proc. Natl. Acad.. Sci.* **2011**, *108* (43), 17791, https://doi.org/doi:10.1073/pnas.1112928108.
[36] B. P. Lomans, A. J. P. Smolders, L. M. Intven, A. Pol, H. J. M. O. denCamp, C. vanderDrift, *Appl. Environ. Microb.* **1997**, *63* (12), 4741, https://doi.org/10.1128/Aem.63.12.4741-4747.1997.
[37] S. Sunagawa, L. P. Coelho, S. Chaffron, et al., *Science* **2015**, *348* (6237), 1261359, https://doi.org/doi:10.1126/science.1261359.
[38] C.-Y. Li, H.-Y. Cao, R. D. Payet, J. D. Todd, Y.-Z. Zhang, *Ann. Rev. Microbiol.* **2024**, *78* (Volume 78, 2024), 513, https://doi.org/https://doi.org/10.1146/annurev-micro-041222-024055.
[39] J. Wilms, J. Lub, R. Wever, *Biochim. Biophys. Acta* **1980**, *589* (2), 324, https://doi.org/10.1016/0005-2728(80)90048-1.
[40] J. Gea, A. Ferrer, R. Monforte, A. Torres, *Med. Clin.* **1986**, *87* (8), 348.

[41] T. Xu, M. Yu, J. Liu, H. Lin, J. Liang, X.-H. Zhang, *Appl. Environ. Microbiol.* **2019**, *85* (7), https://doi.org/10.1128/AEM.02844-18.
[42] A. R. J. Curson, E. K. Fowler, S. Dickens, A. W. B. Johnston, J. D. Todd, *Biogeochemistry* **2012**, *110* (1-3), 109, https://doi.org/10.1007/s10533-011-9663-2.
[43] T. Brettin, J. J. Davis, T. Disz, et al., *Sci. Rep.* **2015**, *5*, 8365, https://doi.org/10.1038/srep08365.
[44] H. Chao, N. Y. Zhou, *J. Bacteriol.* **2013**, *195* (7), 1598, https://doi.org/10.1128/JB.02216-12.
[45] H. C. Gasteiger E., Gattiker A., Duvaud S., Wilkins M.R., Appel R.D., Bairoch A, *The proteomics protocols handbook, Humana press* **2005**, 571.
[46] C.-S. Yu, Y. C. Chen, C.-H. Lu, J.-K. Hwang, *Proteins* **2006**, *64*, https://doi.org/10.1002/prot.21018.
[47] H. Nielsen, K. D. Tsirigos, S. Brunak, G. von Heijne, *Protein J.* **2019**, *38* (3), 200, https://doi.org/10.1007/s10930-019-09838-3.
[48] A. Krogh, B. Larsson, G. von Heijne, E. L. L. Sonnhammer, *J. Mol.. Biol.* **2001**, *305* (3), 567, https://doi.org/10.1006/jmbi.2000.4315.
[49] E. A. Struys, E. E. Jansen, K. de Meer, C. Jakobs, *Clin. Chem.* **2000**, *46* (10), 1650, https://doi.org/10.1093/clinchem/46.10.1650.
[50] J. Klepacki, N. Brunner, V. Schmitz, J. Klawitter, U. Christians, J. Klawitter, *Clin. Chim. Acta* **2013**, *421*, 91, https://doi.org/10.1016/j.cca.2013.03.003.
[51] T. L. M. Stephen F. Altschul, Alejandro A. Schäffer, Jinghui Zhang,, Zheng Zhang, Webb Miller, D. J. Lipman, *Nucleic Acids Res.* **1997**, *25* (17), 3389, https://doi.org/10.1093/nar/25.17.3389.
[52] J. M. Xie, Y. R. Chen, G. J. Cai, R. L. Cai, Z. Hu, H. Wang, *Nucleic Acids Res.* **2023**, *51* (W1), W587, https://doi.org/10.1093/nar/gkad359.
[53] I. M. A. Chen, K. Chu, K. Palaniappan, et al., *Nucleic Acids Res.* **2021**, *49* (D1), D751, https://doi.org/10.1093/nar/gkaa939.
[54] X. Y. Dong, J. E. Rattray, D. C. Campbell, et al., *Nat. Commun.* **2020**, *11* (1), https://doi.org/10.1038/s41467-020-19648-2.
[55] I. Letunic, P. Bork, *Nucleic Acids Res.* **2021**, *49* (W1), W293, https://doi.org/10.1093/nar/gkab301.

Supporting Information

Supporting Information is available from the Wiley Online Library or from the author.

881 **Figure**

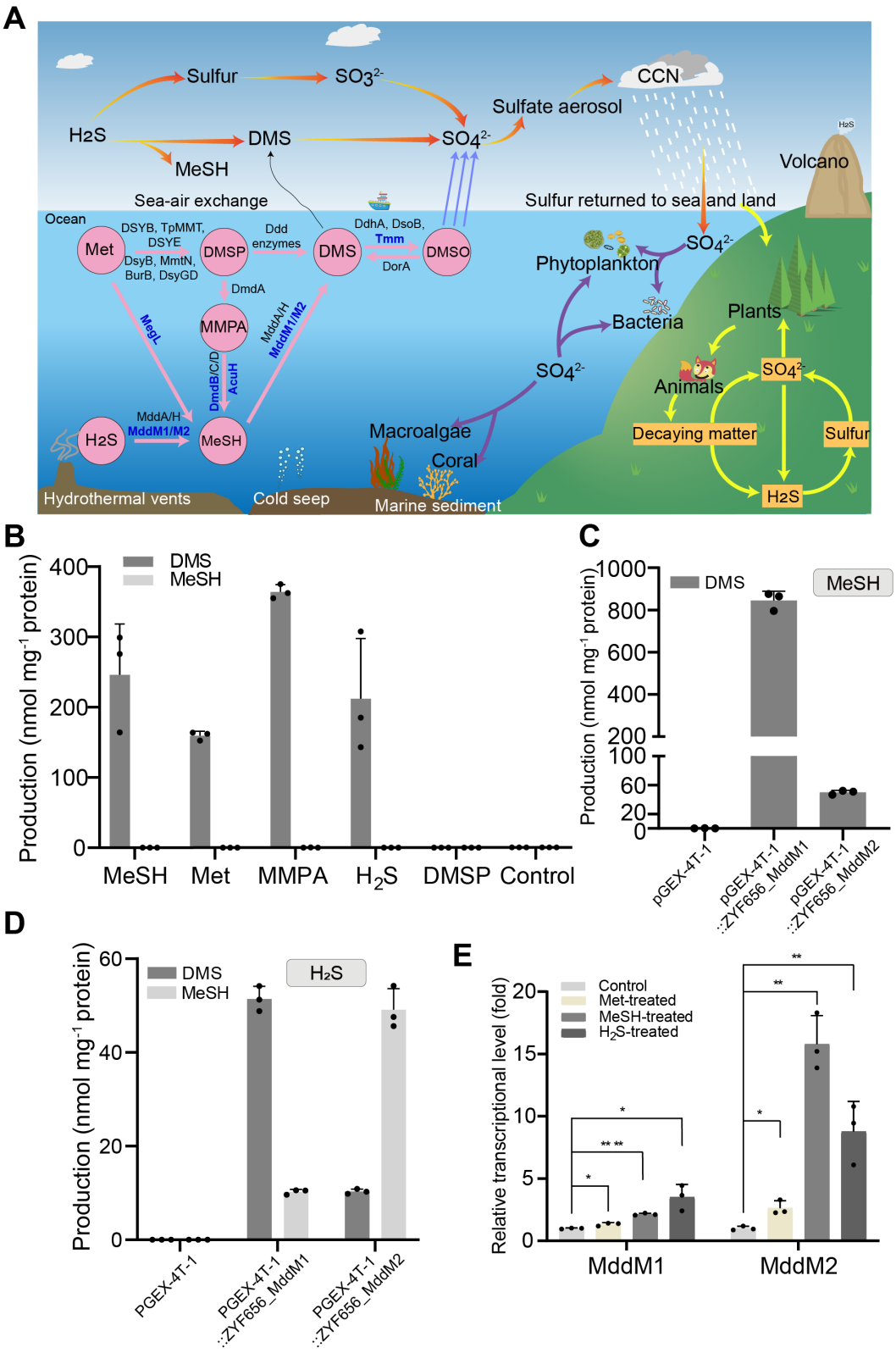

882

883 **Figure 1. Analysis of H_2S and MeSH *S*-methylation by *M. poriferae* ZYF656 and**
884 **its candidate Mdd enzymes. A)** Simplified DMSP/DMS cycle and the key
885 enzymes/pathways involved. Blue fonts predict enzymes/pathways in the strain *M.*

poriferae ZYF656. **B**) Gas chromatography detection of DMS and MeSH produced from *M. poriferae* ZYF656 when incubated with 0.5 mM Met, MeSH, MMPA, H_2S, DMSP or negative control. **C**) DMS production from *E. coli* BL21(DE3) with an empty vector or with clones expressing cloned *mddM1*, *mddM2*, when grown with 0.5 mM MeSH in M9 media. **D**) MeSH and DMS production from *E. coli* containing cloned *mddM1*, *mddM2* or empty vector, when grown with 0.5 mM H_2S in M9 media. **E**) RT-qPCR analyses of *mddM1* and *mddM2* in *M. poriferae* ZYF656 grown with 0.5 mM Met, MeSH or H_2S. The values for DMS and MeSH production are shown as mean ± s.d., and with three biological replicates for each strain. No DMS or MeSH was detected in the blank MBM media control (Data not shown). Significance was determined by Student's *t*-test (**p*<0.05, ***p*<0.01, ****p*<0.001, *****p*<0.0001).

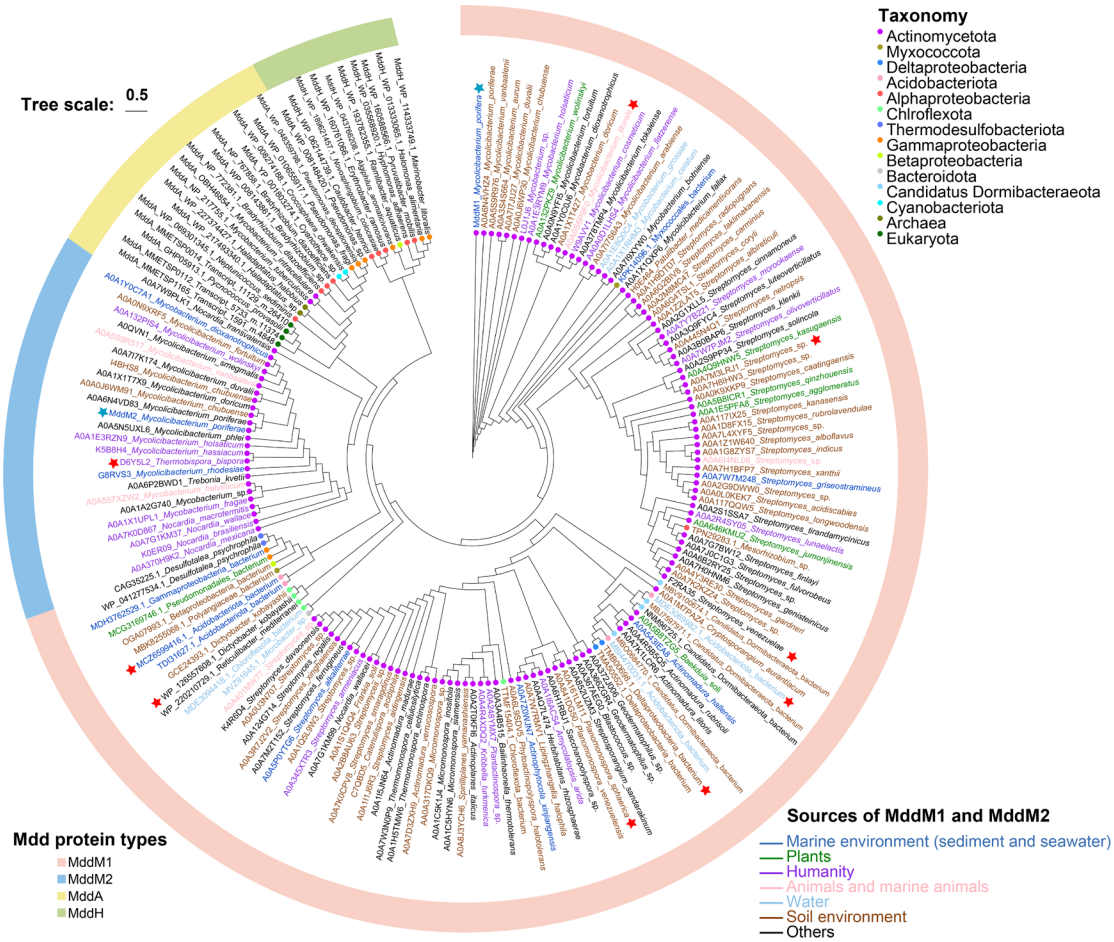

Figure 2. Maximum-likelihood phylogenetic tree of MddM proteins. The tree was constructed using IQ-Tree using the general time reversible model with empirical frequencies and three rates (LG+F+G4), together with the proteins previously shown to have the expected *S*-methyltransferase enzyme activity for DMS production. The scale bar indicates 0.5 amino acid substitutions per site. MddM1 and MddM2 from *M. poriferae* ZYF656 are highlighted by a blue star. Methyltransferase enzymes with experimentally determined Mdd activity were highlighted with a red star. The evolutionary tree uses three distinct color schemes to represent different types of

information: The color blocks around the individual proteins indicate the different Mdd proteins. (See Mdd protein types). The round dots on the branches indicate the taxonomic classification of the bacterial strains (see Taxonomy Key). The color of the leaf labels (organism names) indicates the source of the sequences (see Source Key). The color blocks around the individual proteins indicate the different Mdd proteins.

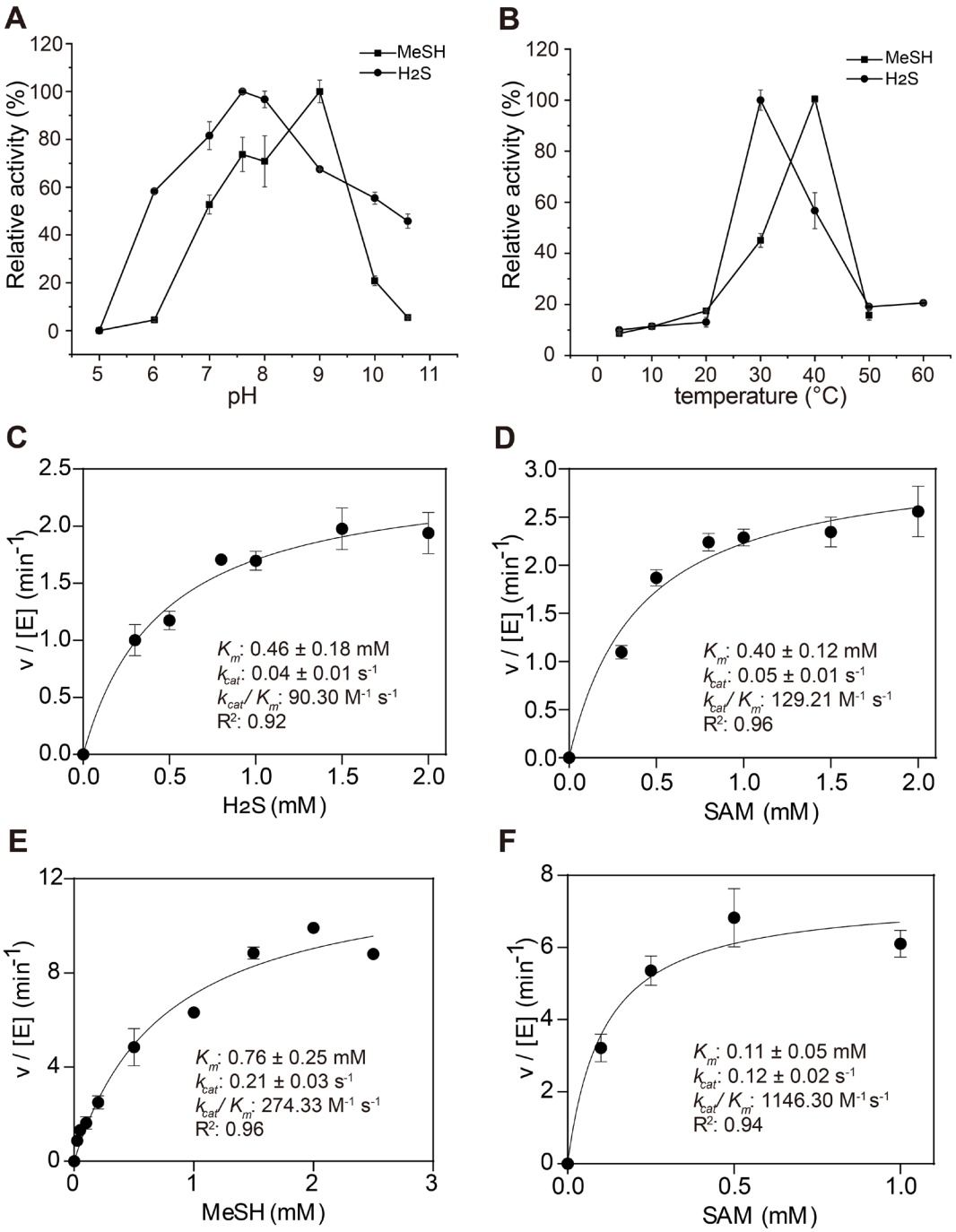

Figure 3. Kinetic characterization of recombinant MddM1. Effect of pH (A) and temperature (B) on the enzymatic activity of MddM1. The 100% activity values correspond to 251.19 and 286.16 nmol mg protein^{-1} min^{-1} for MeSH and H_2S,

respectively, at optimum pH, and to 209.12 and 194.66 nmol mg protein^{-1} min^{-1} at optimum temperature. Substrate-dependence of Mdd1 catalytic activity with varying H_2S concentration (C), or SAM (D)when using H_2S as co-substrate. Assays with H_2S used 1 μg MddM1 at pH 7.5 and 30℃. Substrate-dependence of MddM1 activity with varying MeSH concentration (E), or SAM (F) when using MeSH as co-substrate. Assays with MeSH used 1 μg MddM1 at pH 9.0 and 40℃. Kinetic constants reported in the data panels were obtained by non-linear fitting of data using the rectangular-hyperbola form of the Michaelis-Menten equation, where $v/[E] = k_{cat}\cdot[S]/(K_m + [S])$. The values for DMS production were shown as mean ± s.d. for three biological replicates.

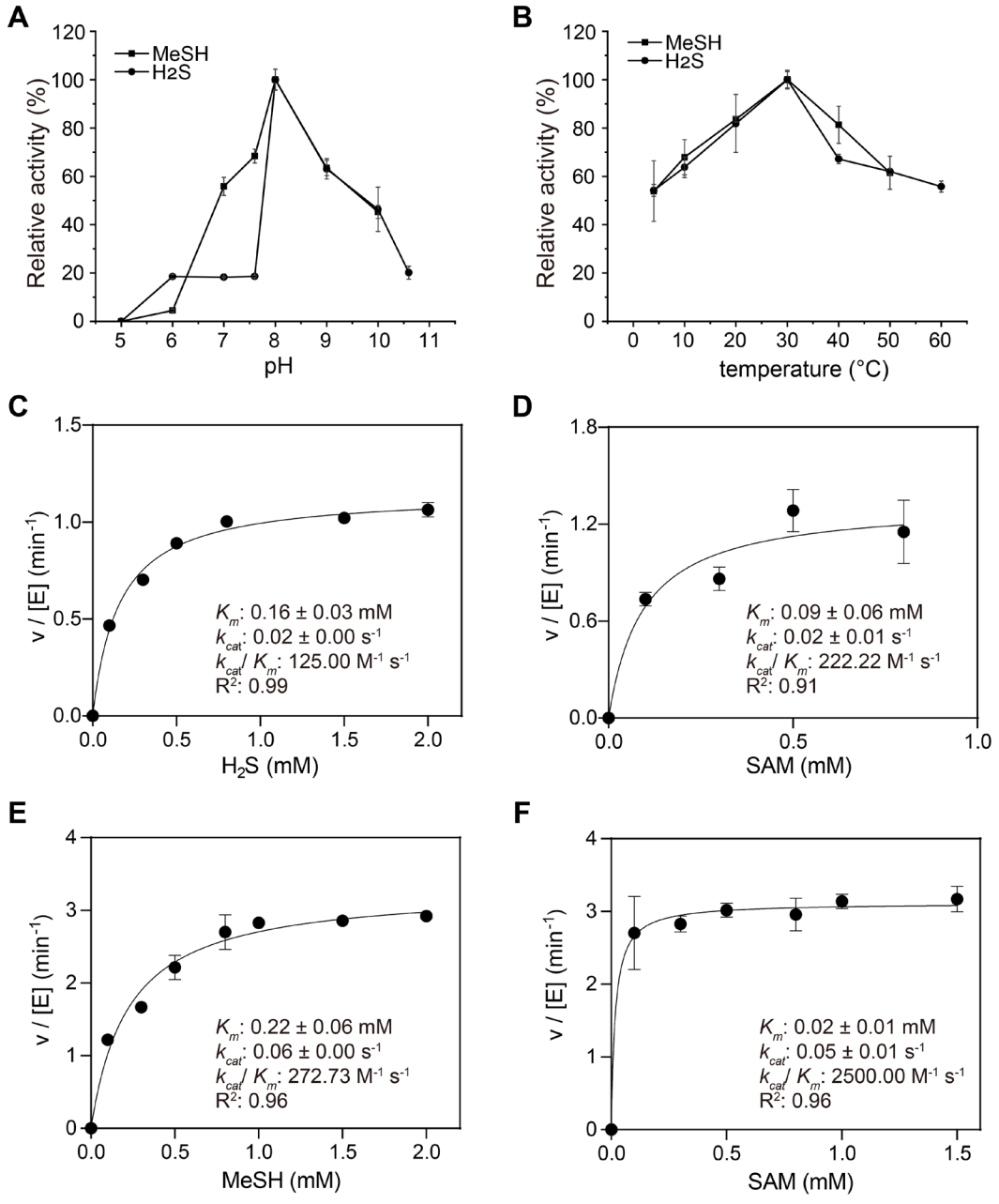

Figure 4. Kinetic characterization of recombinant ^{Tb}MddM2. Effect of pH (A) and temperature (B) on the enzymatic activity of ^{Tb}MddM2. The 100% activity values were 44.73 and 58.73 nmol mg protein^{-1} min^{-1} for MeSH and H_2S, respectively, at optimum pH, and 35.79 and 29.53 nmol mg protein^{-1} min^{-1} at optimum temperature. Substrate-dependence of ^{Tb}MddM2 catalytic activity with varying H_2S concentration (C), or SAM (D) when using H_2S as co-substrate. Substrate-dependence of ^{Tb}MddM2 catalytic activity with varying MeSH concentration (E), or SAM (F) when using MeSH as co-substrate. The kinetic parameters were obtained with 2 µg ^{Tb}MddM2 at pH 8.0 and 30°C. Kinetic constants reported in the data panels were obtained by non-linear fitting of data using the Michaelis-Menten equation as described in Figure 3. The values for DMS production were shown as mean ± s.d. for three biological replicates.

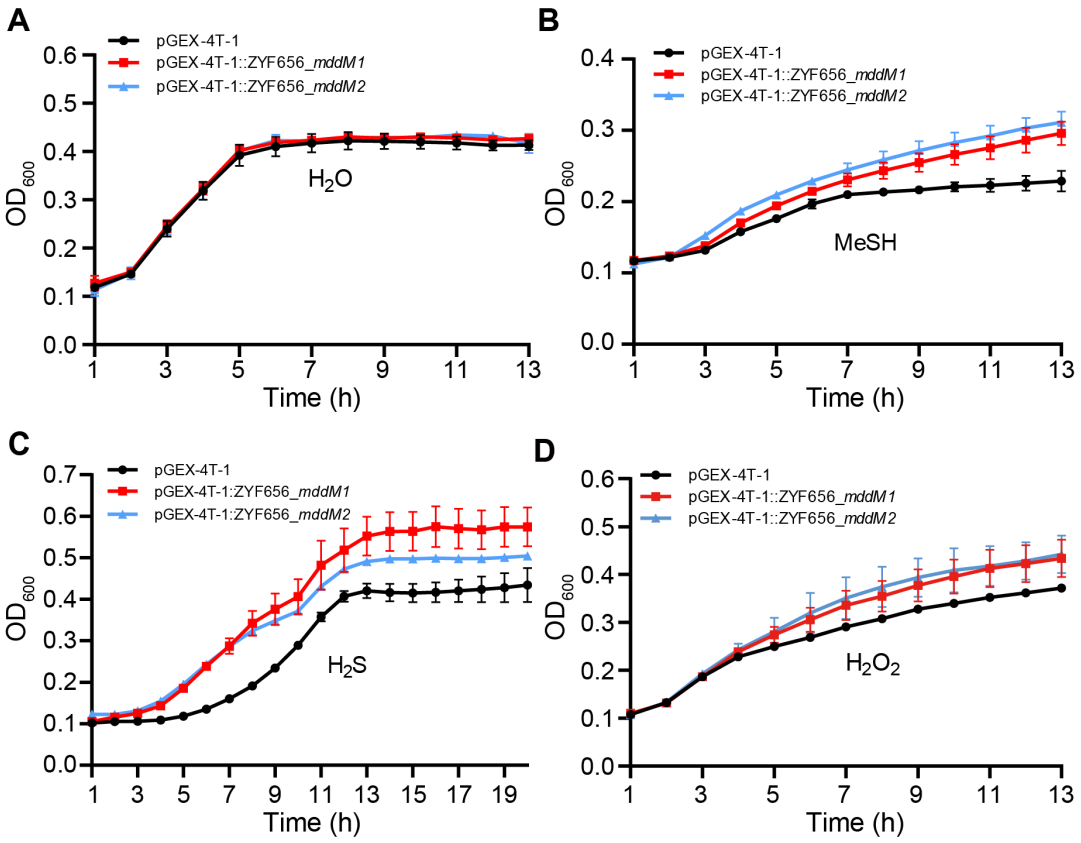

Figure 5. The impact of MddM1 and MddM2 on *E. coli* growth in response to H_2S, MeSH and oxidative stress. A) Growth of *E. coli* strains amended with H_2O (control) in M9 media. B) Growth of *E. coli* strains with 1 mM MeSH in M9 media. C) Growth of *E. coli* strains with 2 mM H_2O_2 in M9 media. D) Growth of *E. coli* strains with 1 mM H_2S in M9 media. Error bars represent the standard deviation from n=3 biological repeats.

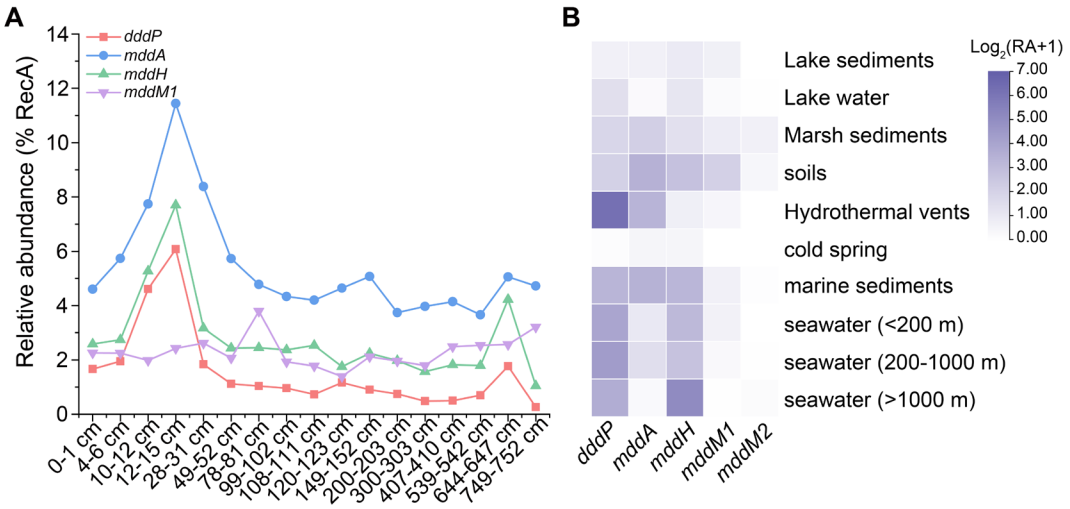

Figure 6. Distribution of *dddP* and *mdd* genes in selected environmental metagenomic datasets. A) Relative abundance of *dddP, mddH, mddA, mddM1* and *mddM2* in a sectioned Mariana Trench sediment core. B) Comparison of the relative abundance of *dddP, mddH, mddA, mddM1* and *mddM2* in different environmental metagenomes. The values represent the logarithm to base 2 of their gene abundance plus 1. RA: relative abundance. The numbers of all sequences were normalized to the number of RecA sequences in each metagenome.

Table 1. Activity of diverse MddH proteins expressed in *E. coli*. Diverse MddM proteins were cloned into pET-24a vector and expressed in *E. coli* BL21 (DE3) grown with 0.5 mM MeSH or with 0.5 mM H_2S. Sequences not highlighted in grey are MddM1 homologues. MddM2 homologue is highlighted in grey.

Accession Number	Source Organism	MeSH	H_2S	
		nmol DMS h^{-1} mg total protein^{-1}	nmol MeSH h^{-1} mg total protein^{-1}	nmol DMS h^{-1} mg total protein^{-1}
MCZ6599416.1	*Acidobacteriota bacterium*	33.23±0.46	33.16±0.82	10.65±0.29
MDE3069982.1	*Acidobacteriota bacterium*	597.19±6.01	27.22±3.73	9.18±0.79
A0A6S6P9F0	*Mycolicibacterium litorale*	107.41±22.41	43.02±3.52	14.57±0.35
TMB00698.1	*Deltaproteobacteria bacterium*	14.29±1.82	112.66±11.25	84.72±9.03
WP_126557608.1	*Dictyobacter kobayashii*	580.93±2.43	45.60±0.52	14.91±1.02
A0A7M3LRJ1	*Streptomyces* sp. SAJ15	26.86±2.88	0	8.79±0.97
A0A161LM11	*Planomonospora sphaerica*	48.97±4.54	30.38±2.89	7.92±0.35
F2RA35	*Streptomyces venezuelae*	76.03±4.16	7.84±0.86	4.89±0.17
D6Y5L2	*Thermobispora bispora*	26.28±0.43	51.77±5.36	7.37±0.16

The values for DMS or MeSH production are shown as mean ± s.d. for three biological replicates.

WILEY-VCH

Supporting Information

Two Novel *S*-methyltransferases Confer Dimethylsulfide Production in *Actinomycetota*

Ruihong Guo, Zihua Guo, Yi Zhou, Yunhui Zhang, Haojin Cheng, Rebecca Devine, Chuang Sun, Ronghua Liu, Yanfen Zheng, Andrew J. Gates, Jonathan D. Todd, Xiao-Hua Zhang**

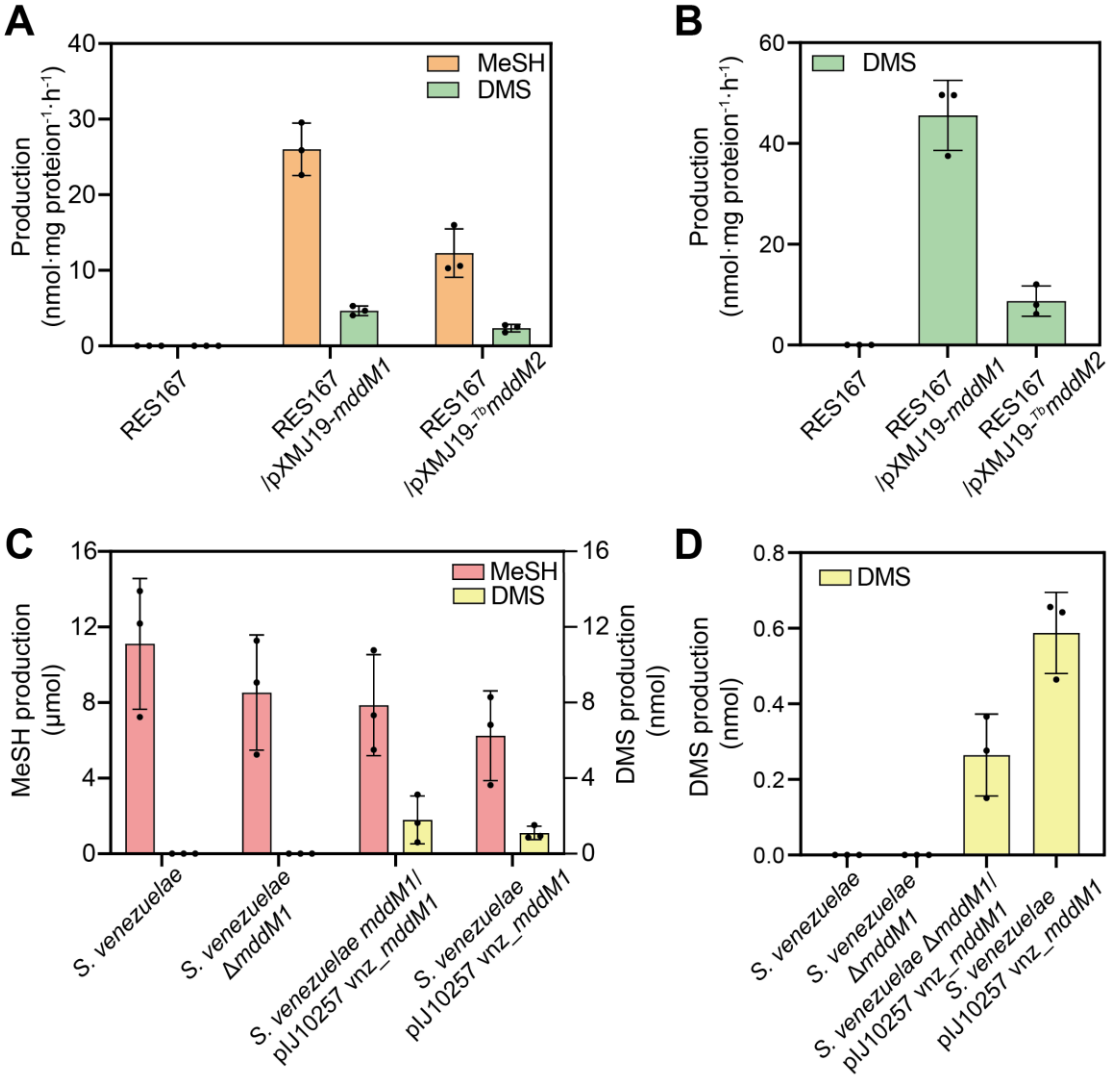

Figure S1. Gas chromatography detection of DMS and MeSH produced from *Corynebacterium glutamicum* RES167, *Streptomyces venezuelae* and their respective mutants. MeSH and DMS production from *C. glutamicum* RES167 containing cloned pXMJ19-*mddM1*, pXMJ19-^{Tb}*mddM2* or empty vector, when grown with 1 mM H_2S (A) or MeSH (B). MeSH and DMS production from *S. venezuelae* wild type and its mutant strains with 1 mM Met (C) or 1 mM H_2S (D). The values for DMS and MeSH production are shown as mean ± s.d.

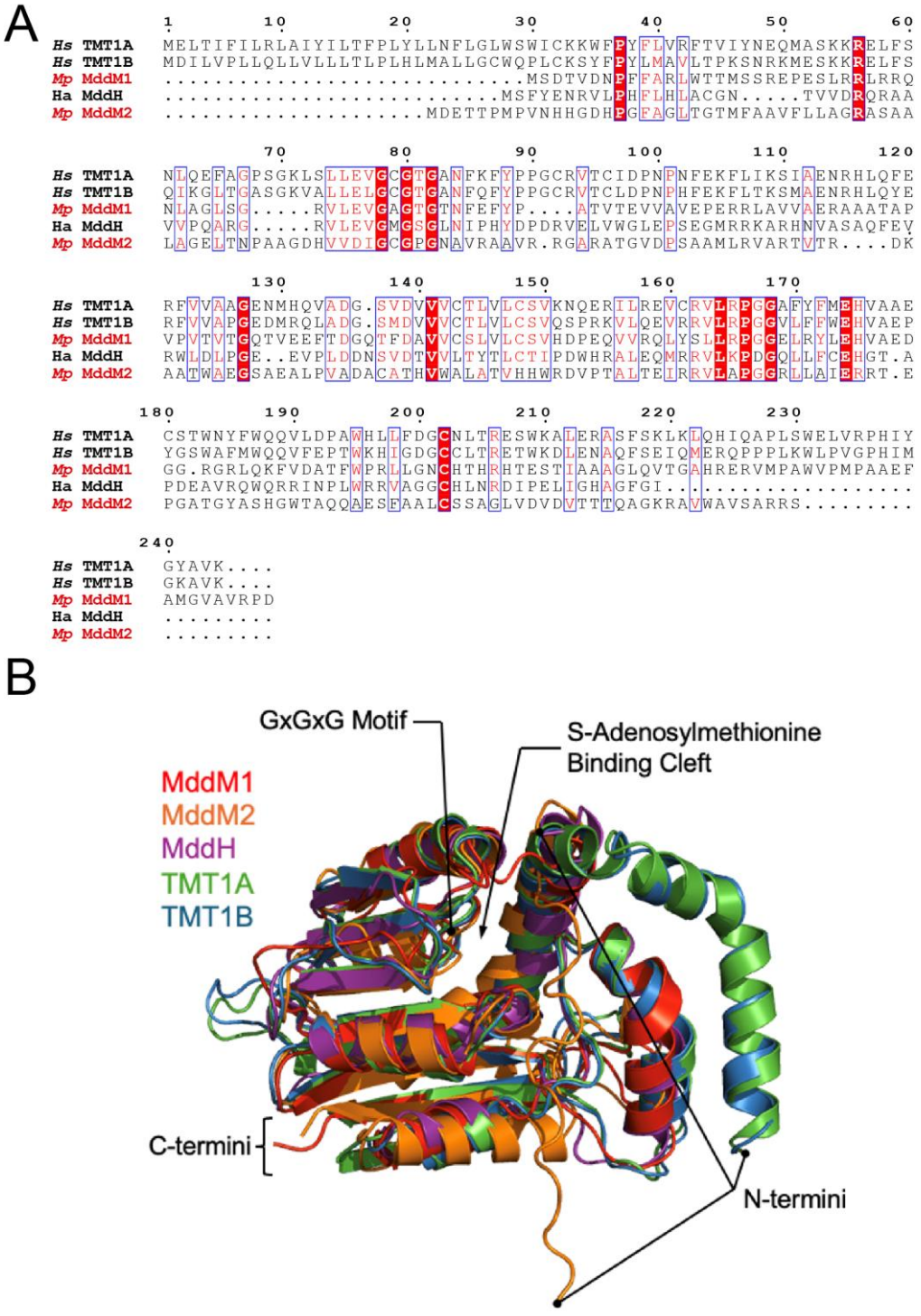

Figure S2. Sequence comparison and structural prediction with other putative and known SAM-dependent methyltransferases. A) Multiple sequence alignment using ClustalW 2.1 and ESPript 3.0. The GxGxG motif and SAM binding cleft are indicated by boxes, and fully conserved residues are highlighted in white on a red background. B) Structural prediction for MddM1 (red), MddM2 (orange), MddH (purple), TMT1A (green) and TMT1B (blue) using AlphaFold3, with the GxGxG motif and SAM-binding cleft annotated. Structural image was generated using Pymol ver 3.0.0.

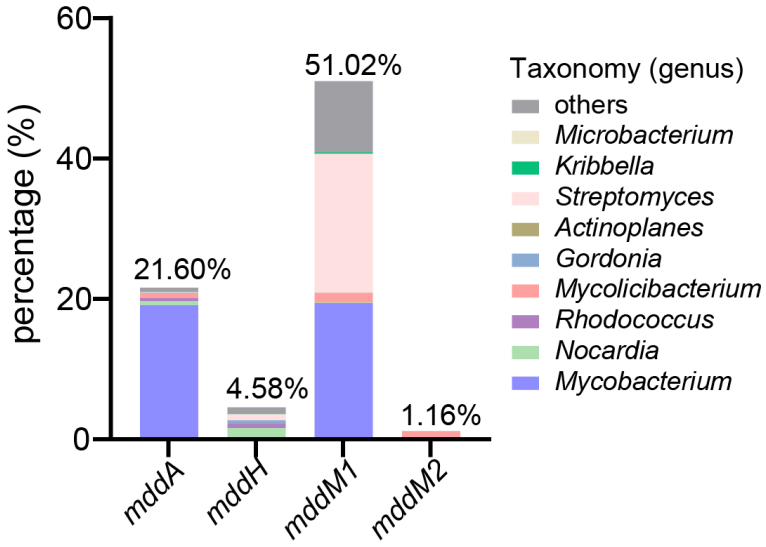

Figure S3. Distribution of *mddA*, *mddH*, *mddM1* and *mddM2* genes in all *Actinomycetota* genomes (n=42,815) downloaded from NCBI.

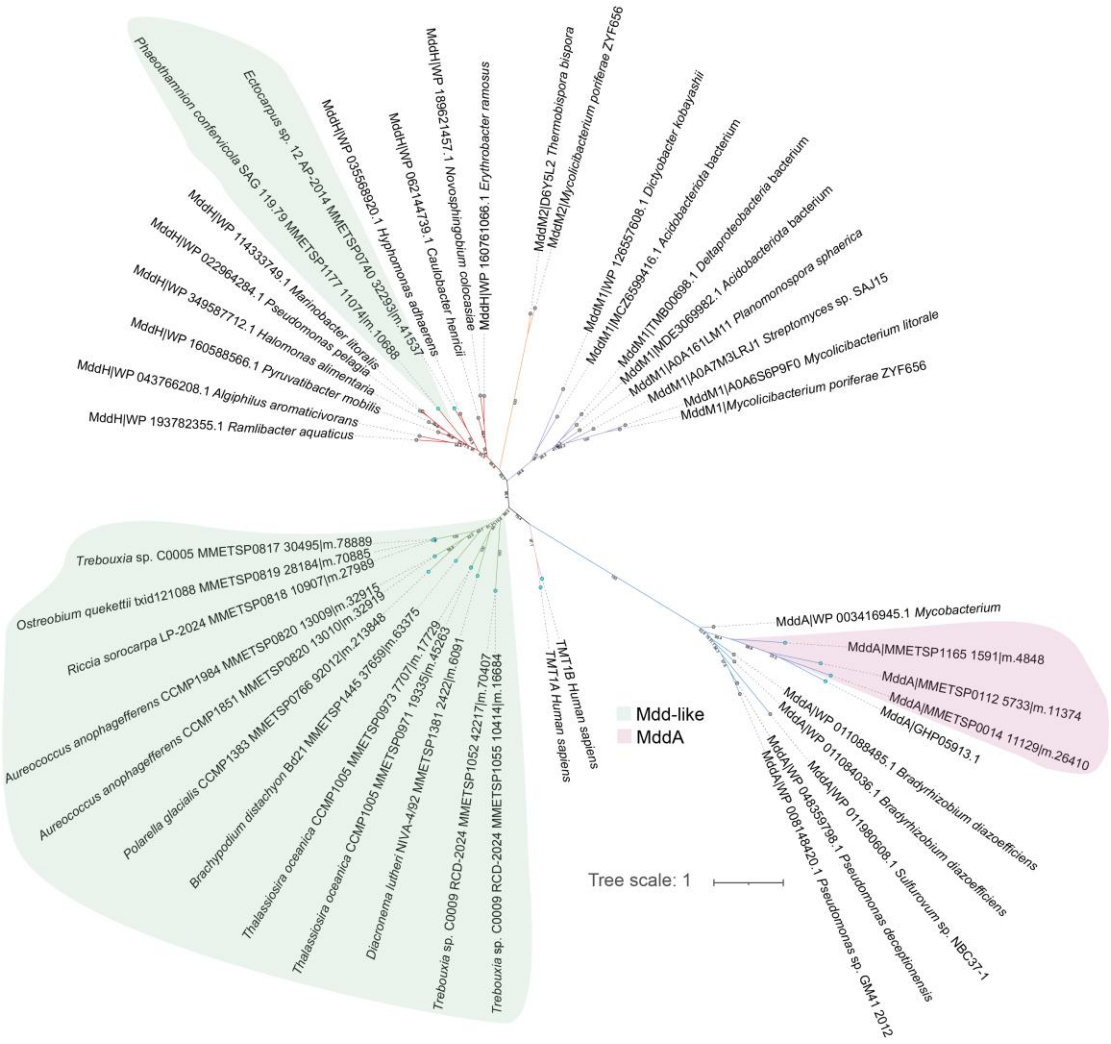

Figure S4. Maximum-likelihood phylogenetic tree of Mdd proteins in eukaryotes. Branches are colored according to different Mdd proteins. Functional MddA sequences in eukaryotes (pink shading) were used as reference sequences. Mdd-like sequences (green shading) indicate matched Mdd proteins in eukaryotes. Lines are colored to distinguish different clusters. Blue and gray dots denote sequences from eukaryotic and prokaryotic organisms, respectively. The scale bar indicates 1 amino acid substitutions per site.

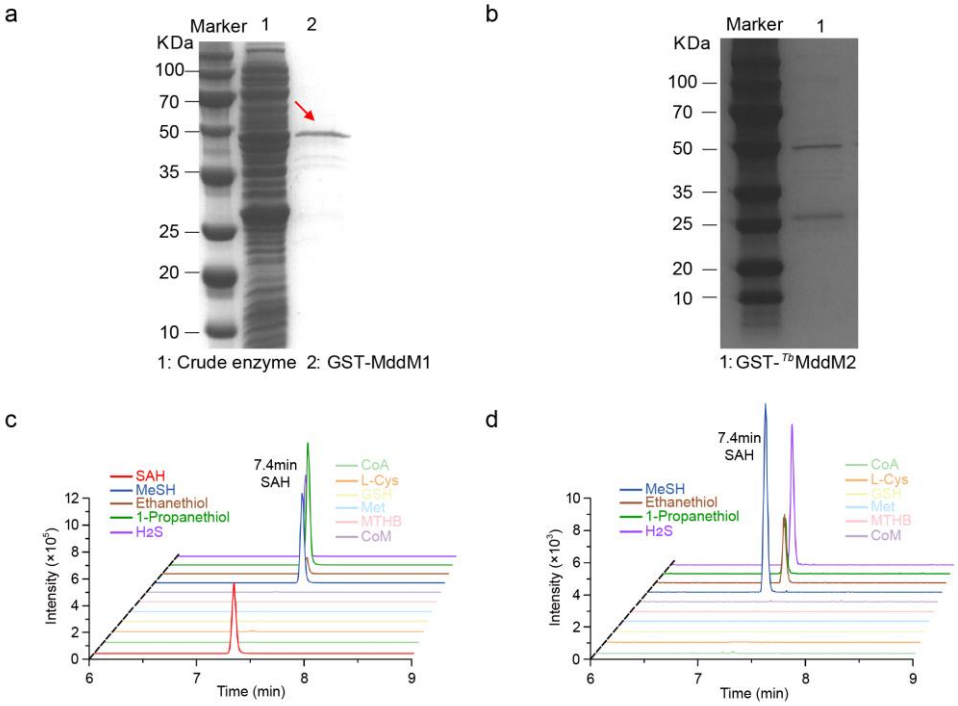

Figure S5. Characterization of the recombinant MddM1 and *Tb*MddM2. A) Properties of purified recombinant GST-tagged MddM1 from *M. poriferae* ZYF656 run on a 12% precast SDS-PAGE gel. Lanes: Marker, prestained protein ladder. Lane 1, lysate before purification; lane 2, purified protein (molecular weight: 50.02 kDa). B) Purified recombinant GST-tagged MddM2 of *Thermobispora bispora*. Lanes: Marker, prestained protein ladder. Lane 1, purified protein (molecular weight: 48.65 kDa). The larger band corresponds to the uncleaved protein, while the smaller band represents the processed form. The ability of MddM1 (C) and *Tb*MddM2 (D) to *S*-methylate a range of substrates (as detailed) as monitored by the formation of *S*-adenosyl-homocysteine (SAH) from *S*-adenosyl-methionine (SAM). MeSH, methanethiol; H_2S, Hydrogen sulfde; CoA, coenzyme A; L-Cys, cysteine; GSH, glutathione; Met, methionine; MTHB, 4-methylthio-2-hydroxybutyrate; CoM, Coenzyme M.

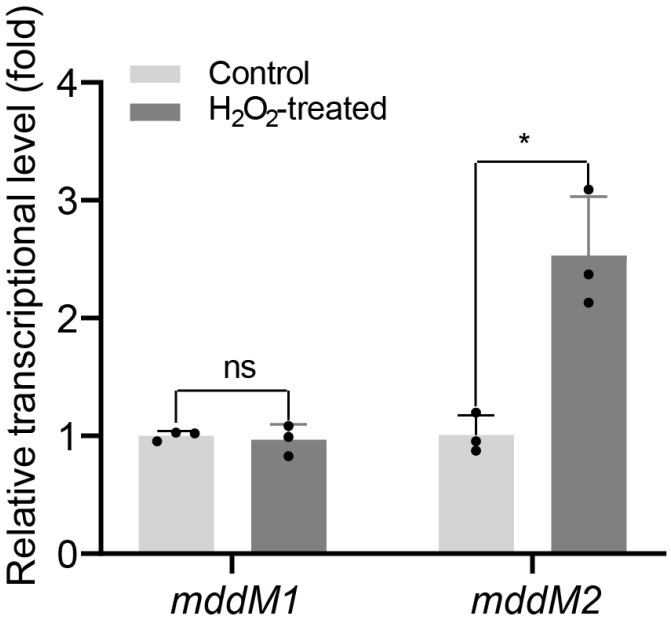

Figure S6. RT-qPCR analyses of *mddM1* and *mddM2* genes of *M. poriferae* ZYF656 in the presence of 2 mM H_2O_2. The values were shown as mean ± s.d. for three biological replicates. Significance was determined by Student's t-test (ns, not significant; *p<0.05).

Table S1. DMS cycling gene analysis of the *M. poriferae* ZYF656 genome by BLASTp against functional gene list.

ZYF656 gene ID	Clostest homologues	Homologue accession ID	Amio acid identity (%)	Evalue	Coverage (%)
PP625016	AcuH	AAV93475.1	64	5.05E-117	99
PP661496	Tmm	ACK52489.1	61	0	100
PP661497	DmdB	WP_011047771.1	51	0	99
PP661492	MegL	AAO46884.1	42	5.77E-100	84

Table S2. Strains and plasmids involved in this study.

Strains or plasmids	Description	Reference or source
Mycolicibacterium poriferae ZYF656	Wild-type isolate; Available from Zhang lab	This study; Zhang Lab
Escherichia coli JM109	recA1 endA1 gyrA96 thi-1 hsdR17 supE44 Δ(lac-proAB/F) [traD36 proAB$^+$ lacIq lacZΔM15]	[1]
E. coli DH5α	Transformed cells for gene cloning	AngYu Biotechnologies (Shanghai, China)
E. coli BL21 (DE3)	Transformed cells for gene expression	AngYu Biotechnologies (Shanghai, China)
pUC18	Plasmid vectors for genomic library in *E. coli* DH5α, ampicillin-resistant	This study; Zhang Lab
pET-24a	Plasmid vector for cloning gene in *E.* coli DH5α, kanamycin-resistant	This study; Zhang Lab
pUCm-T	Plasmid vector for cloning gene in *E. coli* DH5α, ampicillin-resistant	Sangon Biotech
pGEX-4T-1	Plasmid vector for cloning gene in *E. coli* DH5α, ampicillin-resistant	Miaoling Biology
pXMJ19	Plasmid vector for gene expression, chloramphenicol-resistant	This study; Zhang Lab
E. coli NEB5a	fhuA2 Δ(argF-lacZ)U169 phoA glnV44 Φ80 Δ(lacZ) M15 gyrA96 recA1 relA1 endA1 thi-1 hsdR17	New England Biolabs
E. coli ET12567	dam$^-$ dcm$^-$ hsdS$^-$	[2]
pCRISPomyces-2	oriT, reppSG5(ts), oriColE1, sSpcas9, synthetic guide RNA cassette, ampicillin-resistant	[3]
pUZ8002	RK2 derivative with a mutation in oriT, kanamycin-resistant	[4]
pIJ10257	oriT, ΦBT1attB-int, ermEp*, pMS81 backbone, hygromycin B-resistant	[5]
pIJ10257 vnz_mddM1	For the deletion of vnz_mddM1	This study; Jon. Lab
pCRISPomyces-2 vnz_mddM1	For the overexpression of vnz_mddM1	This study; Jon. Lab

Strains or plasmids	Description	Reference or source
pXMJ19::RES167_ *mddM1*	pXMJ19 containing the *mddM1* gene of ZYF656	This study; Zhang Lab
pXMJ19::RES167_ *^{Tb}mddM1*	pXMJ19 containing the *mddM2* gene of *Thermobispora bispora*	This study; Zhang Lab
pGEX-4T-1::ZYF656_*mddM1*	pGEX-4T-1 containing the *mddM1* gene of ZYF656	This study; Zhang Lab
pGEX-4T-1::ZYF656_*mddM2*	pGEX-4T-1 containing the *mddM2* gene of ZYF656	This study; Zhang Lab
pGEX-4T-1::Tb_*MddM2*	pGEX-4T-1 containing the *mddM2* gene of *Thermobispora bispora*	This study; Zhang Lab
S. Venezuelae Δ*mddM1*	knockout strains	This study; Jon. Lab
S. venezuelae/pIJ10257 vnz_*mddM1*	overexpressed strains	This study; Jon. Lab
S. venezuelae ΔmddM1/pIJ10257 vnz_*mddM1*	complementary strains	This study; Jon. Lab

Table S3. Primers used in this study.

Gene name	Primer sequences (5' - 3')	Function and reference
27F	AGAGTTTGATCCTGGCTCAG	the universal primers for bacterial identification.
1492R	GGTTACCTTGTTACGACTT	
mddM1-pGEX4T1-BamHI-F	gatctggttccgcgtggatccATGAGCGACACAGTCGATAATCC	PCR amplification of *mddM1* from ZYF656 and cloning into pGEX-4T-1
mddM1-pGEX4T1-EcoRI-R	ctcgagtcgacccgggaattcTCAGTCCGGCCGCACGGC	
mddM2-pGEX4T1-BamHI-F	gatctggttccgcgtggatccATGGACGAAACCACACCGATG	PCR amplification of *mddM2* from ZYF656 and cloning into pGEX-4T-1
mddM2-pGEX4T1-EcoRI-R	ctcgagtcgacccgggaattcTCAGGACCGGCGCGCGCT	
*Tb*mddM2-pGEX4T1-BamHI-F	gatctggttccgcgtggatccATGAGCGCGGCGGACGTT	PCR amplification of *mddM2* from *Thermobispora bispora* and cloning into pGEX-4T-1
*Tb*mddM2-pGEX4T1-EcoRI-R	ctcgagtcgacccgggaattcCGGACGGGTCGCGGTAAC	
mddM1-pXMJ19-BamHI-F	caggtcgactctagaggatccATGAGCGACACAGTCGATAATCC	PCR amplification of *mddM1* from ZYF656 and cloning into pXMJ19
mddM1-pXMJ19-EcoRI-R	caaaacagccaagctgaattcTCAGTCCGGCCGCACGGC	
*Tb*mddM2-pXMJ19-BamHI-F	caggtcgactctagaggatccATGAGCGCGGCGGACGTT	PCR amplification of *mddM2* from *Thermobispora bispora* and cloning into pXMJ19
*Tb*mddM2-pXMJ19-EcoRI-R	caaaacagccaagctgaattcCGGACGGGTCGCGGTAAC	
ZYF656_*mddM1*-F	tgaggagttcaccgacggt	RT-qPCR amplification of *mddM1*
ZYF656_*mddM1*-R	aaggtcgcgtcgacgaactt	
ZYF656_*mddM2*-F	accacgtcgtcgacatcg	RT-qPCR amplification of *mddM2*
ZYF656_*mddM2*-R	tcgccaatgcccagacgt	
ZYF656_*recA*-F	cagttcctgcagttcaccgt	RT-qPCR amplification of *recA*
ZYF656_*recA*-R	tcacgcagattgggtgacag	

Gene name	Primer sequences (5’ - 3’)	Function and reference
vnz_*mddM1* KO-1F	gctcggttgccgccgggcgtttttaTCTAGAGCTCCGCGAGAGAAG GACACC	*mddM1* deletion flank in *Streptomyces venezuelae*
vnz_*mddM1* KO-1R	GCTGCTGCGACCAGGCGAGCTCGCCGGATGGTGGACA CGGGACG	*mddM1* deletion flank in *S. venezuelae*
vnz_*mddM1* KO-2F	GCGAGCTCGCCTGGTCGCAGCAGCCCGTCGTCGCCGT GCGTCC	*mddM1* deletion flank in *S. venezuelae*
vnz_*mddM1* KO-2R	gcaacgcggccttttacggttcctggccTCTAGACGGTGCCGATGAC GAGCGC	*mddM1* deletion flank in *S. venezuelae*
vnz_*mddM1* gRNA-F	acgcGGCACGTCGAACGCCCGGTA	*mddM1* deletion gRNA in *S. venezuelae*
vnz_*mddM1* gRNA-R	aaacTACCGGGCGTTCGACGTGCC	*mddM1* deletion gRNA in *S. venezuelae*
vnz_*mddM1* test-F	CGTGACGAGCGACGACGACC	*mddM1* test primers in *S. venezuelae*
vnz_*mddM1* test-R	GGACGCACGGCGACGACGG	*mddM1* test primers in *S. venezuelae*
vnz_*mddM1* test INT-F	GGAGGGCAAGACGGTGAAGAACC	*mddM1* test primers in *S. venezuelae*
vnz_*mddM1* test INT-R	CCTTCCAGAAGGCCAGCACG	*mddM1* test primers in *S. venezuelae*
mddM1 pIJ10257-F	gtctagaacaggaggccccatatgCAGACGACCGGGCTGAGGAG	*mddM1* overexpression in *S. venezuelae*
mddM1 pIJ10257-R	ctcatgagaacctaggatccaagcttCGTATCTGAAGATCGGTCATG GCC	*mddM1* overexpression in *S. venezuelae*

Table S4. Accession numbers of the functional ratified enzymes involved in DMS cycling.

Protein	Organism	Accession number
MddM1	*Mycolicibacterium poriferae* ZYF656	PP661493
	Streptomyces sp. SAJ15	A0A7M3LRJ1
	Streptomyces venezuelae	F2RA35
	Dictyobacter kobayashii	WP_126557608.1
	Deltaproteobacteria bacterium	TMB00698.1
	Mycolicibacterium litorale	A0A6S6P9F0
	Acidobacteriota bacterium	MDE3069982.1
	Acidobacteriota bacterium	MCZ6599416.1
	Planomonospora sphaerica	A0A161LM11
MddM2	*Mycolicibacterium poriferae* ZYF656	PP661494
	Thermobispora bispora	D6Y5L2
MddA (EC 2.1.1.334)	*Pseudomonas deceptionensis*	WP_048359798.1
	Mycobacterium tuberculosis H37Rv	NP_217755.1
	Bradyrhizobium diazoefficiens USDA 110 Blr1218	NP_767858.1
	Bradyrhizobium diazoefficiens USDA 110 Blr5741	NP_772381.1
	Cyanothece sp. ATCC 51142	YP_001803274.1
	Bradyrhizobium sp. YR681	WP_008143861.1
	Pseudomonas sp. GM41	WP_008148420.1
	Crocosphaera chwakensis	WP_008274188.1
	Pseudomonas fragi	WP_010655917.1
	Mycobacterium intracellulare	OBH46854.1
	Neptunicoccus sediminis	WP_069301345.1
	Haladaptatus sp. W1	WP_217493340.1
	Haladaptatus sp. PSR5	WP_227374427.1
	Pycnococcus provasolii	GHP05913.1
	Chrysocystis fragilis CCMP3189	MMETSP1165_Transcript_1591|m.4848
	Nitzschia sp. RCC80	MMETSP0014_Transcript_11129|m.26410
	Lotharella globose CCCM811	MMETSP0112_Transcript_5733|m.11374
MddH (EC 2.1.1.-)	*Algiphilus aromaticivorans* DG1253	WP_043766208.1
	Marinobacter litoralis Sw-45	WP_114333749.1
	Pseudomonas pelagia CL-AP6	WP_022964284.1
	Hyphomonas adhaerens MHS-3	WP_035568920.1
	Pyruvatibacter mobilis CGMCC_1.15125	WP_160588566.1
	Novosphingobium colocasiae KCTC 32255	WP_189621457.1
	Erythrobacter ramosus DSM 8510	WP_160761066.1

Protein	Organism	Accession number
	Ramlibacter aquaticus LMG 30558	WP_193782355.1
	Caulobacter henricii CB4	WP_062144739.1
	Halomonas alimentaria EF61	WP_013333065.1
DSYB (EC 2.1.1.373)	*Prymnesium parvum* CCAP946/6	-
	Chrysochromulina tobin CCMP291	KOO32714
	Lingulodinium polyedrum CCMP1936	-
	Alexandrium tamarense ATSP1-B	-
	Acropora cervicornis	-
	Fragilariopsis cylindrus CCMP1102	OEU17621
	Symbiodinium microadriaticum CCMP2467	OLQ07620
TpMMT (EC 2.1.1.67)	*Thalassiosira pseudonana* CCMP1335	Tp23128
DsyB (EC 2.1.1.373)	*Labrenzia aggregata* IAM 12614	WP_006937642
	Labrenzia aggregate LZB033	WP_075282486
	Pseduooceanicola batsensis HTCC2597	WP_009805585
	Pelagibaca bermudensis HTCC2601	WP_007801186
	Sediminimonas qiaohouensis DSM 21189	WP_026756701
	Thalassobaculum salexigens DSM 19539	WP_084618911
	Sagittula stellate E-37	WP_005854984
	Amorphus coralli DSM 19760	WP_018697905
MmtN (EC 2.1.1.-)	*Novosphingobium* sp. MBES04	WP_052321947
	Croceicoccus mobilis	WP_066775518
	Thalassospira sp. HJ	WP_044830103
	Thalassospira sp. MCCC_1A01148	WP_062957385
	Thalassospira indica	WP_064788038
	Thalassospira tepidiphila MCCC_1A03514	WP_064780488
	Thalassospira australica	WP_033070178
	Thalassospira lucentensis	WP_022734010
	Thalassospira sp. MCCC_1A02898	WP_063085993
	Thalassospira profundimaris sp. DSM17430	WP_008888945
	Labrenzia sp. OB1	WP_068409229
	Roseovarius indicus 01	WP_064261696
	Roseovarius indicus 02	WP_057814729
	Roseovarius indicus 03	KRS18724.1
	Rhodobacter aestuarii	WP_076485456
	Saccharothrix syringae	WP_033429235

Protein	Organism	Accession number
	Micromonospora nigra	WP_091090849
	Agrobacterium vitis	WP_071204336
	Nocardiopsis chromatogenes	WP_017624909
	Streptomyces mobaraensis NBRC_13819	EME99407
DmdA (EC 2.1.1.269)	*Ruegeria pomeroyi* DSS-3	AAV95190
	Pelagibacter ubique HTCC1062	WP_011281570
	Dinoroseobacter shibae DFL 12	WP_012178987
	marine gammaproteobacterium HTCC2080	WP_007233625
	Candidatus Pelagibacter sp. HTCC7211	WP_008546106
	Candidatus Puniceispirillum marinum IMCC1322	WP_013044947
DddD (EC 2.8.3.-)	*Marinomonas* sp. MWYL1	ABR72937
	Oceanimonas doudoroffii DSM 7028	AEQ39135
	Psychrobacter sp. J466	ACY02894
	Halomonas sp. HTNK1	ACV84065
	Burkholderia ambifaria AMMD	WP_011659284
	Pseudomonas sp. J465	ACY01992
DddL (EC 4.4.1.3)	*Sulfitobacter* sp. EE-36	ADK55772
	Rhodobacter_sphaeroides	WP_011336734
	Rhodobacter sphaeroides 2.4.1	YP_351475
	Fulvimarina_pelagi	WP_007067665
	Loktanella_vestfoldensis	WP_019955302
	Pseudooceanicola_batsensis	WP_009805827
	Labrenzia aggregata LZB033	AKS25183
	Labrenzia aggregate LZD062	KP639183
DddP (EC 3.4.-.-)	*Roseovarius nubinhibens* ISM	EAP77700
	Ruegeria pomeroyi DSS-3	WP_044029245
	Oceanimonas doudoroffii DSM 7028	AEQ39091
	Oceanimonas doudoroffii DSM 7028	AEQ39103
	Fusarium graminearum PH-1	XP_389272
DddQ (EC 4.4.1.3)	*Ruegeria pomeroyi* DSS-3	WP_011047333
	Roseovarius nubinhibens ISM	EAP76002
	Roseovarius nubinhibens ISM	EAP76001
	Ruegeria lacuscaerulensis ITI-1157	WP_005978225
	GOS databases	ECW91654
	GOS databases	EBP74803
	GOS databases	ECX82089
DddW (EC 4.4.1.3)	*Ruegeria pomeroyi* DSS-3	AAV93771
	Roseobacter sp. MED193	EAQ44306.1
DddY (EC 4.4.1.3)	*Alcaligenes faecalis* M3A	ADT64689
	Shewanella putrefaciens CN-32	ABP77243
	Desulfovibrio acrylicus	SHJ73420

Protein	Organism	Accession number
	Ferrimonas kyonanensis DSM 18153	WP_028114584
	Acinetobacter bereziniae	ENV21217
DddK (-)	*Candidatus Pelagibacter ubique* HTCC1062	AAZ21215
	Alphaproteobacterium HIMB5	AFS47241
	Candidatus Pelagibacter ubique HTCC9022	WP_028037226
	Pelagibacteraceae bacterium BACL20 MAG-120920-bin64	KRP06000
	Candidatus Pelagibacter ubique	WP_006997514
	Candidatus Pelagibacter ubique	WP_027306832
	Candidatus Pelagibacter ubique	WP_018413735
Almal (EC 4.4.1.3)	*Emiliania huxleyi* CCMP1516	XP_005784450
	Emiliania huxleyi CCMP1516	XP_005763983
	-	sp|P0DN22
DddX (-)	*Psychrobacter* sp. (56811)	7CM9_1
	Psychrobacter sp. P11G5	WP_068035783
	Sporosarcina sp. P33	WP_081242855
	Roseobacteraceae	WP_109384856
	Marinobacterium jannaschii	WP_084332639
DddU (-)	*Ruegeria faecimaris* DSM 28009	WP_142638590.1
	Phaeobacter inhibens P66	WP_058277181.1
	Aliiroseovarius pelagivivens KCTC 42459	WP_108856353.1
	Pseudaestuariivita atlantica MCCC 1A09432	WP_050532617.1
	Amylibacter cionae H-12	WP_188671731.1
	Shimia sediminis ZQ172	WP_127114513.1
	Leisingera aquimarina DSM 24565	WP_027260001.1
AcuH (EC 4.2.1.17)	*Ruegeria lacuscaerulensis* ITI-1157	EEX08788.1
	Ruegeria pomeroyi DSS-3	AAV93475.1
DmdB (EC 6.2.1.44)	*Ruegeria pomeroyi*	WP_011047771
	Ruegeria pomeroyi	WP_011046428
	Candidatus Pelagibacter ubiqu	WP_011281571
DmdC (EC 1.3.99.41)	*Ruegeria pomeroyi*	WP_011049476
	Burkholderia thailandensis	WP_009892931
	Ruegeria lacuscaerulensis ITI-1157	EEX10128
	Ruegeria pomeroyi	WP_011048615
	Pseudomonas	WP_003114720
	Pseudomonas	WP_003114561
	Burkholderia thailandensis	WP_009889880
	Ruegeria lacuscaerulensis ITI-1157	EEX08676
DmdD	*Ruegeria pomeroyi* DSS-3	Q5LLW6.1

Protein	Organism	Accession number
(EC 4.2.1.155)		
DorA (-)	*Rhodobacter Capsulatus*	1DMR_A
DsoB (EC 1.14.13.245)	*Acinetobacter sp.*	BAA23331.1
Tmm (EC 1.14.13.148)	*Ruegeria pomeroyi* DSS-3	AAV94838.1
	Methylophaga aminisulfidivorans	WP_007144064
	Methylocella silvestris BL2	ACK52489.1
	Roseovarius sp. 217	EAQ26624.1
	Candidatus Pelagibacter ubique HTCC1002	EAS85405.1
	Candidatus Pelagibacter sp. HTCC7211	EDZ59919.1
DdhA (EC 1.8.5.3)	*Sagittula stellata* E-37	EBA07058.1
	Rhodovulum sulfidophilum	AAN46632.1
DmoA (EC 1.14.13.131)	*Hyphomicrobium sulfonivorans*	6AK1_A
MTO (EC 1.8.3.4)	*Hyphomicrobium* sp.	ATJ26742.1
	Methylophaga thiooxydans	WP_008290534
	Ruegeria pomeroyi	WP_011242048
	Hyphomicrobium denitrificans ATCC 51888	ADJ22562.1
	Pseudovibrio ascidiaceicola	WP_093522951
	Methylococcus capsulatus str. Bath	AAU90430.1

Table S5. List of candidates MddM proteins with their accession numbers.

Organism and enzymes	Candidate protein	Accession number	Length (aa)	Identity (%)	Evalue	Coverage (%)
Streptomyces sp. SAJ15	MddM1	A0A7M3LRJ1	224	47	2e-58	98
Planomonospora sphaerica	MddM1	A0A161LM11	219	48	8e-44	97
Acidobacteriota bacterium	MddM1	MCZ6599416.1	220	42.23	1e-30	95
Acidobacteriota bacterium	MddM1	MDE3069982.1	216	43.6	3e-39	99
Mycolicibacterium litorale	MddM1	A0A6S6P9F0	209	68.4	7.41e-94	100
Deltaproteobacteria bacterium	MddM1	TMB00698.1	216	47.47	8e-49	99
Dictyobacter kobayashii	MddM1	WP_126557608.1	213	41.12	3e-31	90
Streptomyces venezuelae	MddM1	F2RA35	221	47.4	4.21e-45	94
Thermobispora_bispora	MddM2	D6Y5L2	204	58.6	8.4e-80	99

Table S6. Protein sequences used in the molecular phylogenetic analysis of MddM proteins.

Strain	Accession number	Identity (%)	Evalue	Coverage (%)
Mycolicibacterium llatzerense	A0A0D1LHS4	66	7.17E-90	98
Mycolicibacterium chubuense	A0A0J6WP30	77.5	8.45E-110	97
Streptomyces caatingaensis	A0A0K9XKP9	46	4.15E-44	98
Streptomyces acidiscabies	A0A0L0KEK7	45.5	4.05E-43	96
Mycolicibacterium fortuitum	A0A0N9YFI5	70.9	7.80E-100	99
Streptomyces sp.	A0A0U3N707	42.9	4.13E-44	94
Streptomyces kanasensis	A0A117IX25	46.3	4.27E-46	93
Streptomyces longwoodensis	A0A117QQW5	44.5	4.06E-43	93
Streptomyces regalis	A0A124G714	43	3.95E-41	92
Mycolicibacterium wolinskyi	A0A132PKZ9	73.7	7.89E-101	96
Planomonospora sphaerica	A0A161LM11	48.1	3.99E-42	93
Micromonospora siamensis	A0A1C5HYN6	49	4.48E-49	98
Micromonospora inositola	A0A1C5K1J4	49	4.37E-48	99
Streptomyces rubrolavendulae	A0A1D8FX15	44.5	4.12E-44	93
Mycobacterium holsaticum	A0A1E3RYM9	72.2	7.87E-101	100
Streptomyces agglomeratus	A0A1E5PFA8	44.3	3.99E-42	91
Mycobacterium grossiae	A0A1E8Q0C4	70.7	7.38E-93	95
Streptomyces indicus	A0A1G8ZYS7	43.1	4.12E-44	96
Thermomonospora echinospora	A0A1H5TMW6	44.9	4.13E-44	96
Streptomyces radiopugnans	A0A1H9DTD7	45.5	3.97E-42	96
Streptomyces aidingensis	A0A1I1J6R3	44.7	4.10E-44	95
Actinomadura madurae	A0A1I5JN64	44.9	4.11E-44	89
Amycolatopsis arida	A0A1I6ACS4	42.9	3.86E-40	99

Strain	Accession number	Identity (%)	Evalue	Coverage (%)
Cryptosporangium aurantiacum	A0A1M7PAZ4	47.8	4.48E-49	97
Streptomyces sp.	A0A1Q5L9W3	46.2	4.27E-46	94
Frankia soli	A0A1S1Q4Q4	46.7	4.24E-46	95
Mycolicibacterium fallax	A0A1X1QXP6	66.7	7.15E-90	99
Mycobacterium celatum	A0A1X1RHM3	68.9	7.40E-94	98
Mycobacterium doricum	A0A1X1T427	68.9	7.62E-97	99
Mycobacterium dioxanotrophicus	A0A1Y0C0J6	68.3	7.53E-96	97
Streptomyces alboflavus	A0A1Z1W640	43.3	3.92E-41	92
Streptomyces albireticuli	A0A1Z2LAT5	44.3	4.21E-45	92
Plantactinospora sp.	A0A248YMX7	50.7	4.50E-50	98
Streptomyces sp.	A0A2B8AU63	45.9	4.27E-46	95
Streptomyces cinnamoneus	A0A2G1XLL5	46	4.13E-44	92
Streptomyces sp.	A0A2G9DWW0	43.1	3.99E-42	96
Streptomyces carminius	A0A2M8MC47	50	4.34E-47	93
Streptomyces lunaelactis	A0A2R4SY05	42.7	3.95E-41	94
Streptomyces tirandamycinicus	A0A2S1SSA7	44.5	3.93E-41	93
Streptomyces solincola	A0A2S9PP34	45.5	4.24E-46	99
Actinoplanes italicus	A0A2T0KFI6	46.9	4.31E-47	94
Micromonospora sp.	A0A317DKQ9	48.3	4.41E-48	99
Streptomyces armeniacus	A0A345XTR3	46	4.38E-48	96
Geodermatophilus sp.	A0A366ZGR4	48.3	4.41E-48	96
Blastococcus sp.	A0A367AEG0	50.2	4.40E-48	95
Geodermatophilus sp.	A0A372J006	54.6	4.55E-51	95
Mycolicibacterium tokaiense	A0A378TMP4	69.8	7.19E-91	100

Strain	Accession number	Identity (%)	Evalue	Coverage (%)
Bailinhaonella thermotolerans	A0A3A4B515	48.3	4.46E-49	98
Streptomyces klenkii	A0A3B0BAP6	46	4.16E-44	85
Streptomyces luteoverticillatus	A0A3Q9FYC4	46.7	4.27E-46	93
Streptomyces xinghaiensis	A0A3R7J2V2	44.2	4.19E-45	93
Mycolicibacterium aurum	A0A3S4S664	78.9	8.59E-112	99
Streptomyces sp.	A0A401MW77	44.2	4.31E-47	92
Streptomyces netropsis	A0A445N4Q1	45.8	4.26E-46	93
Herbihabitans rhizosphaerae	A0A4Q7L474	47.5	4.03E-43	84
Streptomyces kasugaensis	A0A4Q9HNW5	44.5	4.07E-43	95
Kribbella turkmenica	A0A4R4XDQ2	46.2	3.98E-42	96
Actinomadura rubrisoli	A0A4R5B5Q5	46.3	4.23E-46	99
Streptomyces gardneri	A0A4Y3RE30	46.4	4.07E-43	95
Actinomadura hallensis	A0A543IEA8	49.8	4.19E-45	99
Streptomyces qinzhouensis	A0A5B8ICR1	47.2	4.39E-48	88
Baekduia soli	A0A5B8TZG5	49.5	3.83E-40	88
Streptomyces alkaliterrae	A0A5P0YTG6	44.7	4.31E-47	94
Mycolicibacterium vanbaalenii	A0A5S9R976	79.4	8.85E-116	99
Streptomyces jumonjinensis	A0A646KMU2	44.5	4.28E-46	93
Streptomyces sp.	A0A6B2RY25	45	4.02E-42	93
Streptomyces taklimakanensis	A0A6G2BIV8	48.1	4.15E-44	95
Streptomyces coryli	A0A6G4TSL1	46	4.03E-43	95
Saccharopolyspora sp.	A0A6H1RBJ1	46.1	4.08E-43	97
Streptomyces sp.	A0A6I4NL08	43.3	4.05E-43	94
Phytoactinopolyspora halotolerans	A0A6L9SDV5	47.6	4.44E-49	99

Strain	Accession number	Identity (%)	Evalue	Coverage (%)
Mycolicibacterium poriferae	A0A6N4VHZ4	97.1	1.06E-141	100
Mycolicibacterium litorale	A0A6S6P9F0	68.4	7.41E-94	100
Actinomadura verrucosospora	A0A7D3ZXH9	45.9	4.21E-45	94
Nocardia wallacei	A0A7G1KM99	46.8	4.02E-42	91
Streptomyces finlayi	A0A7G7BW12	44.1	4.11E-44	94
Streptomyces genisteinicus	A0A7H0HNM6	49.3	4.42E-48	95
Streptomyces xanthii	A0A7H1BFP7	46.2	4.25E-46	95
Streptomyces sp.	A0A7H8IHW3	43.9	4.22E-45	91
Mycolicibacterium duvalii	A0A7I7JU27	76.4	8.14E-105	99
Mycolicibacterium arabiense	A0A7I7S6A3	71.5	7.82E-100	98
Mycobacterium botniense	A0A7I9XYW0	65.4	7.33E-93	97
Streptomyces fulvorobeus	A0A7J0C1G3	44.1	4.13E-44	91
Streptomyces smaragdinus	A0A7K0CPV8	44.1	4.11E-44	97
Actinomadura litoris	A0A7K1LCR6	43.6	4.04E-43	99
Streptomyces sp.	A0A7K2KZZ4	45.9	4.02E-42	92
Streptomyces sp.	A0A7L4XYF5	46.4	6.20E-48	95
Streptomyces ferrugineus	A0A7M2T152	45.5	4.31E-47	100
Streptomyces sp.	A0A7M3LRJ1	46.7	4.44E-49	94
Thermomonospora cellulosilytica	A0A7W3N0P9	45.4	4.11E-44	96
Streptomyces griseostramineus	A0A7W7M248	44.6	3.92E-41	92
Streptomyces olivoverticillatus	A0A7W7PJM2	46.4	4.33E-47	93
Lipingzhangella halophila	A0A7W7RMV1	46.9	4.27E-46	98
Streptomyces morookaense	A0A7Y7B221	45	4.20E-45	93
Actinophytocola xinjiangensis	A0A7Z0WJN7	44.9	3.91E-41	96

Strain	Accession number	Identity (%)	Evalue	Coverage (%)
Planomonospora venezuelensis	A0A841DG50	46.8	4.07E-43	94
Streptosporangium sandarakinum	A0A852UZM3	46.9	4.16E-45	99
Spirilliplanes yamanashiensis	A0A8J3YCH6	49.3	4.43E-49	98
Catenulispora acidiphila	C7QBD5	44.4	3.88E-40	93
Streptomyces venezuelae	F2RA35	47.4	4.21E-45	94
Patulibacter medicamentivorans	H0E464	49.8	4.97E-57	99
Streptomyces davaonensis	K4R6D4	44	4.26E-46	91
Mycobacterium sp.	L0J1J6	72.7	7.81E-100	98
Mycolicibacterium cosmeticum	W9AVV1	67.8	7.40E-94	100
Myxococcales bacterium	KPK14096.1	65.57	3.00E-79	86
Candidatus Dormibacteraeota bacterium	MBV9100674.1	48.8	3.00E-52	98
Deltaproteobacteria bacterium	TMB00698.1	47.47	8.00E-49	99
Acidobacteriota bacterium	MBI4470031.1	47.57	6.00E-48	96
Deltaproteobacteria bacterium	TMA50552.1	47.47	2.00E-47	99
Mesorhizobium sp.	TPN29283.1	44.76	5.00E-44	98
Chloroflexota bacterium	TMF15404.1	44.39	8.00E-41	96
Acidobacteriota bacterium	MDE3069982.1	43.6	3.00E-39	99
Candidatus Dormibacteraeota bacterium	MBJ7597971.1	47.09	1.00E-37	80
Chloroflexota bacterium	MDE3094418.1	41.84	1.00E-33	90
Candidatus Dormibacteraeota bacterium	MBO0684770.1	46.67	3.00E-33	83
Desulfotalea psychrophila	WP_041277534.1	41.81	3.00E-32	81
Pseudomonadales bacterium	MCG3169746.1	44.07	4.00E-32	81
Desulfotalea psychrophila	CAG35225.1	41.81	6.00E-32	81
Reticulibacter mediterranei	WP_220210729.1	43.01	1.00E-31	85

Strain	Accession number	Identity (%)	Evalue	Coverage (%)
Polyangiaceae bacterium	MBK8255068.1	43.09	2.00E-31	83
Betaproteobacteria bacterium	OGA07993.1	42.63	2.00E-31	87
Dictyobacter kobayashii	WP_126557608.1	41.12	3.00E-31	90
Microbacter sp.	MVZ91645.1	43.81	4.00E-31	90
Acidobacteriota bacterium	TDI31627.1	43.16	1.00E-30	87
Acidobacteriota bacterium	MCZ6599416.1	42.23	1.00E-30	95
Candidatus Dormibacteraeota bacterium	NNM96725.1	44.26	2.00E-30	86
Candidatus Dormibacteraeota bacterium	MDA8393919.1	40.29	4.00E-30	96
Dictyobacter kobayashii	GCE24393.1	43.18	8.00E-30	80
Mycolicibacterium chubuense	A0A0J6WM91	67	7.01E-88	90
Mycolicibacterium fortuitum	A0A0N9XRF5	61.2	6.47E-80	97
Mycolicibacterium wolinskyi	A0A132PIS4	60.9	1.4E-80	98
Mycobacterium sp.	A0A1A2G740	61.2	1.00E-80	96
Mycobacterium holsaticum	A0A1E3RZN9	62.3	7.2E-86	99
Mycobacterium doricum	A0A1X1T7X9	65.8	5.4E-86	98
Mycobacterium fragae	A0A1X1UPL1	56.7	5.80E-70	96
Mycobacterium dioxanotrophicus	A0A1Y0C7A1	61.2	2.8E-80	97
Nocardia mexicana	A0A370H9K2	57.3	1.9E-71	98
Mycobacterium helveticum	A0A557XZW2	55.7	2.5E-58	99
Mycolicibacterium phlei	A0A5N5UXL6	57.9	6.02E-75	95
Mycolicibacterium vanbaalenii	A0A5S9R517	66	1.6E-94	99
Mycolicibacterium poriferae	A0A6N4VD83	94.1	7.9E-138	99
Trebonia kvetii	A0A6P2BWD1	50.8	3.4E-60	94
Nocardia wallacei	A0A7G1KM37	52.7	4.5E-65	99
Mycolicibacterium duvalii	A0A7I7K174	61.9	1.6E-82	99
Nocardia macrotermitis	A0A7K0D867	51.2	3.2E-65	99
Nocardia transvalensis	A0A7W9PLK1	55.1	1.2E-66	98
Mycolicibacterium smegmatis	A0QVN1	59	8.5E-78	97
Thermobispora bispora	D6Y5L2	58.6	8.4E-80	99
Mycolicibacterium rhodesiae	G8RVS3	59.9	6.41E-79	97
Mycobacterium chubuense	I4BHS8	65.8	6.8E-91	99
Nocardia brasiliensis	K0ER09	53.8	5.31E-62	96

Strain	Accession number	Identity (%)	Evalue	Coverage (%)
Mycolicibacterium hassiacum	K5B8H4	59.9	6.21E-76	93
Mycolicibacterium poriferae	ZYF656_4275U	32.231	1.24E-09	54

Table S7. Environmental metagenomes used in this study.

Metagenome	Genome ID	Gene count
Seawaters (<200 m)	3300021365 3300017799 3300020175 3300023086 3300021416 3300032691 3300037872 3300032559 3300032630 3300035205 3300024336 3300032480 3300037871 3300032673	
Seawaters (200-1000 m)	3300040813 3300037866 3300028045 3300023276 3300027861 3300022916 3300037802 3300037870 3300037801 3300027996 3300040814 3300035163 3300035206 3300035100 3300023112	51,527,838
Seawaters (>1000 m)	3300035403 3300037621 3300035400 3300035404 3300034629 3300034654 3300037581 3300035399 3300037573 3300034655 3300037557 3300035402 3300034628 3300035401 3300035286	
Marine sediment	3300009788 3300034302 3300037450	50,135,914

Metagenome	Genome ID	Gene count
	3300038548	
	3300037246	
	3300005590	
	3300027828	
	3300005920	
	3300009529	
	3300027967	
	3300024263	
	3300038629	
	3300034301	
Lake water	3300045144	8,514,210
	3300029268	
	3300021092	
	3300043465	
	3300045010	
	3300044987	
	3300045018	
	3300020220	
	3300043775	
	3300037829	
	3300031884	
	3300032881	
	3300045009	
Lake sediment	3300035198	6,922,166
	3300031999	
	3300016621	
	3300036761	
	3300031834	
	3300016581	
	3300016609	
Marsh sediment	3300031643	2,753,065
	3300031351	
	3300037399	
	3300031537	
	3300031585	
	3300031653	
	3300031276	
	3300031551	
Soils	3300020795	6,333,561
	3300020909	
	3300026481	
	3300043690	
	3300030606	
	3300034170	
	3300036859	
	3300036827	
Hydrothermal vent	3300019457	383,001
	3300019450	

Metagenome	Genome ID	Gene count
	3300019455	
	3300019447	
	3300019452	
	3300019446	
	3300019453	
	3300019448	
	3300019443	
	3300019439	
	3300019440	
	3300019456	
	3300019454	
	3300019451	
	3300019395	
Cold spring	SRR12623522 (S7) SRR12623521 (S6) SRR12623520 (S5) SRR12623519 (S4)	11,423,434

Reference

1. C. Yanisch-Perron, J. Vieira, and J. Messing, Improved M13 phage cloning vectors and host strains: nucleotide sequences of the M13mp18 and pUC19 vectors. *Gene*, 1985. 33(1): 103-19.
2. D. J. MacNeil, J. L. Occi, K. M. Gewain, et al., Complex organization of the Streptomyces avermitilis genes encoding the avermectin polyketide synthase. *Gene*, 1992. 115(1-2): 119-25.
3. R. E. Cobb, Y. Wang, and H. Zhao, High-efficiency multiplex genome editing of Streptomyces species using an engineered CRISPR/Cas system. *ACS Synthetic Biology*, 2015. 4(6): 723-8.
4. S. Sioud, B. Aigle, I. Karray-Rebai, et al., Integrative Gene Cloning and Expression System for Streptomyces sp. US 24 and Streptomyces sp. TN 58 Bioactive Molecule Producing Strains. *BioMed Research International*, 2009. 2009(1): 464986.
5. H.-J. Hong, M. I. Hutchings, L. M. Hill, M. J. Buttner, The Role of the Novel Fem Protein VanK in Vancomycin Resistance in Streptomyces coelicolor. *Journal of Biological Chemistry*, 2005. 280(13): 13055-13061.